

Minimal Realizations of Dirac Neutrino Mass from Generic One-loop and Two-loop Topologies at $d = 5$

Sudip Jana,^a Vishnu P.K.,^b Shaikh Saad^b

^a*Max-Planck-Institut für Kernphysik, Saupfercheckweg 1, 69117 Heidelberg, Germany*

^b*Department of Physics, Oklahoma State University, Stillwater, OK 74078, USA*

E-mail: sudip.jana@mpi-hd.mpg.de, vipadma@okstate.edu,
shaikh.saad@okstate.edu

ABSTRACT: We carry out a systematic investigation for the minimal Dirac neutrino mass models emerging from generic one-loop and two-loop topologies that arise from $d = 5$ effective operator with a singlet scalar, σ . To ensure that the tree-level Dirac mass, as well as Majorana mass terms at all orders, are absent for the neutrinos, we work in the framework where the Standard Model is supplemented by the well-motivated $U(1)_{B-L}$ gauge symmetry. At the one-loop level, we analyze six possible topologies, out of which two of them have the potential to generate desired Dirac neutrino mass. Adopting a systematic approach to select minimal models, we construct seventeen viable one-loop Dirac neutrino mass models. By embracing a similar methodical approach at the two-loop, we work out twenty-three minimal candidates. Among the forty selected economical models, the majority of the models proposed in this work are new. In our search, we also include the scenarios where the particles in the loop carry charges under the color group. Furthermore, we discuss the possible dark matter candidates within a given model, if any, without extending the minimal particle content.

Contents

1	Introduction	1
2	Search for minimal one-loop models	5
2.1	Generic topologies, nomenclature and adopting viable topologies	5
2.2	Search for minimal one-loop models without colored particles	7
2.3	Search for minimal one-loop models with colored particles	11
3	Search for minimal two-loop models	14
3.1	Generic topologies, nomenclature and selecting viable skeleton diagrams	14
3.2	Search for minimal two-loop models without colored particles	15
3.3	Search for minimal two-loop models with colored particles	24
4	Possible dark matter candidates	25
5	Conclusions	26

1 Introduction

The Standard Model (SM) of particle physics has been a very successful theory to explain the observed universe at the microscopic level. Despite its great triumph, the SM is unable to explain several observed phenomena, among them, the observation of neutrino oscillations is considered to be the biggest drawback of the SM. Neutrinos are still the least understood of all the fundamental particles discovered so far. The origin of the neutrino oscillations must be linked to new physics beyond the SM (BSM), hence finding the mechanism responsible for neutrino mass generation is of greatest importance. However, to attempt to find a mechanism behind the neutrino mass, the first obstacle the theorists encounter is the unknown nature of the neutrinos. In principle, neutrinos can be Majorana or Dirac type in nature, with no theoretical preference toward either of the possibilities. Most of the proposals in the literature assume that neutrinos are Majorana¹ in nature, whereas mass generation mechanisms for Dirac² type neutrinos are less studied and deserve further attention. In the last several years, there have been growing interests³ in model building, assuming Dirac nature of the neutrinos.

¹Implementation of seesaw mechanisms for generating Majorana neutrino masses are proposed in Refs. [1–7] and radiative mass models for Majorana neutrinos are introduced in Refs. [8–12]. For a recent review on Majorana neutrino mass models see Ref. [13].

²The first radiative neutrino mass model was proposed in Ref. [14], assuming Dirac nature for the neutrinos.

³For construction of Dirac neutrino mass models by employing seesaw mechanisms see for example Refs. [15–31]. For works on radiative Dirac neutrino mass models see for example Refs. [32–59].

If neutrinos are Dirac particles, the theory must contain the right-handed neutrinos ν_R , which are singlets under the SM. As a result, one can write down the following $d = 4$ renormalizable term in the Lagrangian:

$$\mathcal{L}_4 = -y_{ij}^\nu \bar{L}_i \tilde{H} \nu_{Rj} + h.c., \quad (1.1)$$

here, $L = (\nu_L \ell_L^-)^T$ is the SM lepton doublet, $H = (H^+ H^0)^T$ is the SM Higgs doublet, $\tilde{H} = \epsilon H^*$ (ϵ is the 2-index Levi-Civita tensor) and $i, j = 1 - 3$ correspond to generation indices. Note that when the electroweak (EW) symmetry is spontaneously broken by the vacuum expectation value (VEV) of H , the $d = 4$ term given in Eq. (1.1) gives Dirac mass to the neutrinos at the tree-level. However, from the neutrino oscillation data, this demands that the associated Yukawa couplings must be extremely small, $y^\nu \sim \mathcal{O}(10^{-11})$. Due to this small Yukawa couplings, this possibility is expected not to be natural [60]. Instead, it is aesthetically attractive, to generate Dirac mass for the neutrinos radiatively that allows natural values of the Yukawa coupling as a result of the loop suppression. Implementation of such a mechanism requires additional symmetries BSM to forbid the tree-level mass term given in Eq. (1.1), as well as Majorana neutrino mass terms at all orders. In principle, this additional symmetry can be discrete or continuous, global or local in nature. In the literature, many different symmetries [32–59] are considered to forbid these unwanted mass terms.

Though many of the works assume global symmetries to prohibit undesirable terms, from the theoretical grounds, introducing a local symmetry is more appealing. It is because the local symmetries are known to be respected by gravitational interactions [61–65], whereas global symmetries are not. Motivated by this feature of local symmetries, in this work we extend the SM with gauged $U(1)_{B-L}$ symmetry [66–69]. Here B and L correspond to baryon and lepton numbers respectively. The introduced $U(1)_{B-L}$ symmetry not only serves the purpose of forbidding the aforementioned unwanted terms, but also it offers a rich phenomenology and is considered as one of the most economical gauge extensions of the SM. However, in this work we do not focus on the associated phenomenology that are well studied in the literature⁴, rather focus on neutrino mass generation mechanisms utilizing $U(1)_{B-L}$ symmetry. It should be pointed out that the results of this work remain unchanged regardless of the nature (global or local) of this symmetry.

It is well known that $U(1)_{B-L}$ gauge extension of the SM with three right-handed neutrinos is anomaly free. Between two possible anomaly free $B - L$ charge assignments [71–73] of the right-handed neutrinos: $\nu_{R1,2,3} = \{-1, -1, -1\}$ and $\nu_{R1,2,3} = \{5, -4, -4\}$, only the latter is able to serve our purpose. Hence we adopt the second solution in this work. Consequently, the $d = 4$ term of Eq. (1.1) is forbidden, and we consider the following $d = 5$ effective operator for neutrino mass generation:

$$\mathcal{L}_5 = -\frac{h_{ij}}{\Lambda} \bar{L}_i \tilde{H} \nu_{Rj} \sigma + h.c., \quad (1.2)$$

here, the neutral scalar σ is a singlet under the SM and we assign it three units of $B - L$ charge, as a result, $h_{i1} = 0$. The quantum numbers of all the SM particles, the right-handed neutrinos, and the scalar singlet σ under $SM \times U(1)_{B-L}$ are listed in Table 1.

⁴For a review see for example Ref. [70].

Multiplets	$SU(3)_C \times SU(2)_L \times U(1)_Y \times U(1)_{B-L}$
Quarks	$Q_{L_i}(3, 2, \frac{1}{6}, \frac{1}{3})$ $u_{R_i}(3, 1, \frac{2}{3}, \frac{1}{3})$ $d_{R_i}(3, 1, -\frac{1}{3}, \frac{1}{3})$
Leptons	$L_i(1, 2, -\frac{1}{2}, -1)$ $\ell_{R_i}(1, 1, -1, -1)$ $\nu_{R_i}(1, 1, 0, \{5, -4, -4\})$
Higgs	$H(1, 2, \frac{1}{2}, 0)$ $\sigma(1, 1, 0, 3)$

Table 1: Quantum numbers of the SM particles, the right-handed neutrinos and the singlet scalar σ .

In this work, we aim to systematically search for the minimal models to generate Dirac neutrino mass radiatively by utilizing the $d = 5$ effective operator given in Eq. (1.2). We construct generic topologies emerging from this $d = 5$ operator at the one-loop and two-loop levels and, build the associated minimal models. Whereas, only a few of these models resulting from our comprehensive systematic construction exist in the literature, however, most of the models presented in this work are new. Minimal one-loop and two-loop models resulting from our exhaustive search to be discussed at length are summarized in Tables 2, 3, 4 and 5. Whereas a systematic classification of Majorana neutrino mass mechanisms and identifying minimal models are extensively discussed in the literature [74–83], similar analysis for the case of Dirac neutrinos are still lacking. Along this direction, some recent attempts are taken: a systematic classification of tree-level and one-loop mass mechanisms at $d = 4$ [84], $d = 5$ [85, 86], $d = 6$ [87, 88], two-loop mass models at $d = 4$ [84, 89], selecting minimal models at one-loop [49] and identifying simplest models at one-loop, two-loop and three-loop [53] are considered.

In our search strategy, *minimality* refers to finding a model among many different possibilities such that it has the following features:

- It consists of minimum number of BSM states.
- $SU(2)_L$ singlet BSM states are preferred. If BSM particles are required not to be iso-singlets, then we minimize the number of states that are charged under $SU(2)_L$.
- If a particle is charged under $SU(2)_L$, then the lowest dimensional representation is preferred. We impose the same rule in scenarios, where a particle carry $SU(3)_C$ charge.
- If possible, introduction of any BSM fermion is prohibited.
- For a model, where the presence of BSM fermionic state is required, we assume it to be vector-like under $SM \times U(1)_{B-L}$ so that it does not alter the aforementioned anomaly-free conditions.

Moreover, whenever fermionic extension is required, we always assume it comes with three generations and Dirac type in nature. When building a one-loop model, for the neutrinos

it must not contain any tree-level mass term, and similarly, for a two-loop model, both tree-level and one-loop diagrams must be absent. A model can only be called a *true model*, once these criteria are met. Here we point out that, in this set-up, due to non-universal charge assignment of the right-handed neutrinos, one of the neutrinos will always remain massless, which however is completely consistent with neutrino oscillation data. Whereas by further extension of each of the models can accommodate non-zero mass for all the neutrino states, and can be done straightforwardly, for the sake of minimality we do not discuss such possibilities here.

In identifying minimal models emerging from generic one-loop and two-loop topologies, we first construct models by employing BSM fields that do not carry any color. Then we extend our search involving colored particles as well. By explicit construction, we demonstrate that for some of the models with colored particles in the loop, an analogous version with color-singlet states does not exist, or vice versa. For the desired neutrino mass mechanism to realize, we employ scalar leptoquarks, di-quarks and colored fermions depending on the specific model. Some of these colored particles appear in various BSM theories such as grand unified theories⁵ (GUTs) [93–98], technicolor models [99–101], other compositeness scenarios [102], R-parity violating supersymmetric models [103], and dark matter models [104]. Utilization of the colored particles in building Majorana neutrino masses are extensively considered by extending the particle content of the SM, see for example Refs. [13, 105]. Colored particles have also received further attention in view of the possibilities to explain certain striking discrepancies observed in the flavor sector. Models with scalar leptoquarks can explain the discrepancies observed mostly in rare decay modes of B mesons by various experimental collaborations, like Belle, LHCb and BaBar. However, there is no literature where colored scalars and/or fermions are introduced in the context of Dirac neutrino mass generation mechanism. For the first time, we are presenting radiative models where colored particles, especially leptoquarks are employed to generate tiny Dirac neutrino masses. The discovery of the leptoquarks would be an unambiguous signal of this kind of BSM physics and hence, various searches for such particles were conducted in the past experiments and the hunt is still ongoing at the current collider experiments.

Furthermore, for all minimal models proposed in this work, we investigate possibilities of the existence of dark matter (DM) candidates within the working framework, without extending the minimal particle content. Our analysis shows that for majority of the proposed models, the presence of the DM particles can arise naturally due to the appearance of residual dark symmetry resulting from spontaneously broken $U(1)_{B-L}$ group. Hence, these models can explain two seemingly uncorrelated phenomena, the origin of neutrino mass and observed DM in the universe, under the same umbrella.

The paper is organized as follows. In Section 2, we scrutinize the possible one-loop topologies and construct the minimal Dirac neutrino mass models emerging from them. In Section 3, we investigate the two-loop possibilities and build the associated economical Dirac neutrino mass models from the generic topologies. We also investigate the possible dark matter candidates within the minimal one-loop and two-loop models in section 4.

⁵For the origin of neutrino mass from simple GUTs, see for example Refs. [90–92].

Finally we conclude in Section 5.

2 Search for minimal one-loop models

In this section, we systematically build minimal one-loop models in the framework introduced in Sec. 1. First, we discuss the procedure of selecting relevant topologies from which minimal models can be constructed.

2.1 Generic topologies, nomenclature and adopting viable topologies

Let us first define our convention. In this work, we denote each of the one-loop topologies by T1-x, where 1 unambiguously stands for one-loop and x ($x = i, ii, iii, \dots$) is used to differentiate among the different possible topologies. From each of these topologies, specifying the Lorentz structure can lead to multiple diagrams. If there exist more than one diagram within a fixed topology T1-x, we label them as T1-x-y (with $y = 1, 2, 3, \dots$) and furthermore, associated with a diagram T1-x-y, since multiple models can be fabricated by varying the quantum numbers of the internal particles, we name model diagrams as T1-x-y-z (where $z = A, B, C, \dots$). That is, a *topology* T1-x does not contain the Lorentz nature, whereas a *diagram*, T1-x-y is formed from a *topology* by specifying the Lorentz nature of the propagators. Furthermore, from a *diagram* T1-x-y, we construct specific models by assigning quantum numbers of each of the particles within the *diagram* and call them *model diagrams* T1-x-y-z. Whereas, the number of *topologies* and *diagrams* are finite, but infinite number of *model diagrams* can be generated starting from a fixed *topology*. However, we only focus on identifying the most economical *model diagrams* emerging from each individual *topology*.

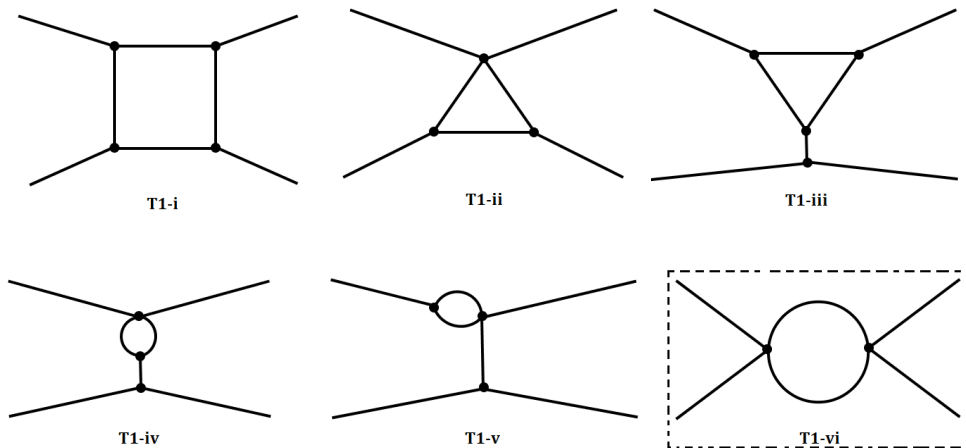


Figure 1: All possible topologies at the one-loop with four external legs. The topology inside the black dashed box leads to non-renormalizable models.

Without further ado, we now conduct a systematic search to find minimal one-loop models. Following the diagrammatic approach, one can find out all possible one-loop topologies associated with four external legs [77], which are listed in Fig. 1 after discarding the

self-energy-like diagrams. However, not all the topologies listed in Fig. 1 can lead to successful one-loop neutrino masses due to various reasons to be discussed below. First, note that in our scenario, two of the external legs must be fermions for any of the topologies listed above. As a result, the topology T1-vi, corresponds to non-renormalizable operator, hence we eliminate it immediately.

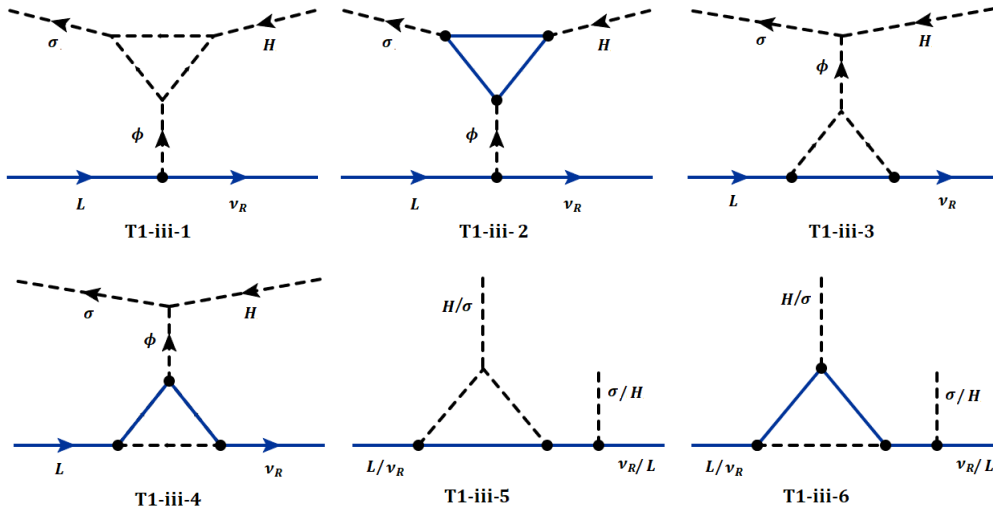


Figure 2: One loop diagrams arising from topology T1-iii.

Till now the Lorentz nature of each line is not specified. To proceed further we specify the spinor and scalar nature of the propagators. First, we focus on the T1-iii topology, which leads to six different diagrams that can be categorized as: (a) diagram with all three internal fermion (or scalar) propagators, (b) diagram with two internal fermion propagators, (c) diagram where only one of the three internal states is a fermion. All these six possible diagrams are presented in Fig. 2. From these diagrams, one immediately sees that T1-iii- y with $y=1-4$, all contain the same scalar ϕ attached to the external fermion (scalar) lines in diagrams T1-iii-1,2 (T1-iii-3,4). In all these models, regardless of the other particles circulating in the loop, the quantum number of this scalar is uniquely fixed to be $\phi(1, 2, -\frac{1}{2}, 3)$ by either the external fermion or scalar fields. As a result, in the Lagrangian, a cubic term of the form $\mathcal{L} \supset H\phi\epsilon\sigma^* \supset H^0\phi^0\sigma^{0*}$ is allowed, which leads to an induced VEV of the neutral component of ϕ after both the $U(1)_{B-L}$ and EW symmetries are broken. Consequently, neutrinos receive a tree-level mass from the $d = 4$ renormalizable term: $\mathcal{L} \supset y \bar{L}\phi\nu_R$ that is invariant under the entire gauge symmetry, $\text{SM} \times U(1)_{B-L}$. Hence we discard these four⁶ diagrams T1-iii- y with $y=1-4$.

Before discussing the T1-iii-5,6 possibilities, here we leave a brief remark cornering topologies T1-iv,v. For these topologies to provide renormalizable models, the lower two external particles must be fermions. In such a scenario, it is now straightforward from the

⁶It is worthwhile to point out that depending on the model, fermionic mass insertions or scalar mixings are required inside the loop for these diagrams to be convergent.

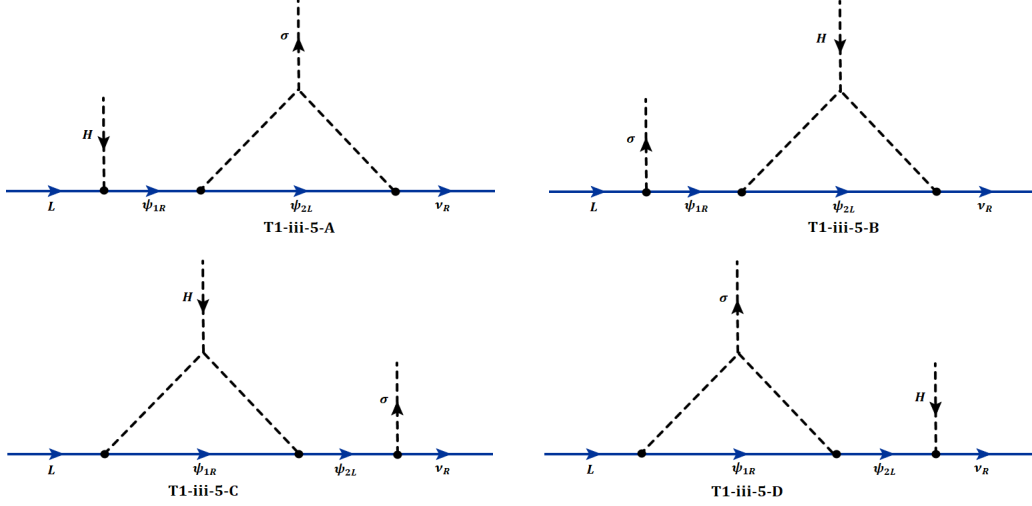


Figure 3: Variations of the one loop diagrams of the type T1-iii-5.

above discussion to realize that constructing models out of these two topologies demand the same scalar field $\phi(1, 2, -1/2, 3)$, hence generate neutrino mass at tree-level and fail to qualify to be a true radiative model.

Let us now discuss the second last diagram T1-iii-5 listed in Fig. 2. From this, different variations of diagrams can be constructed by swapping the external Higgs doublet and singlet which are presented in Fig. 3. It is straightforward to try to build models associated with each of these four types of diagrams. However, here we show that none of these diagrams leads to any successful radiative model. To get an understanding, first, consider the T1-iii-5-A model diagram. From the leftmost vertex, the quantum number of the fermion fields $\psi_{1L,R}$ is automatically fixed to be $(1, 1, 0, -1)$, without specifying the quantum numbers of the rest of the particles in the loop. Introduction of such a fermion leads to the following terms in the Lagrangian:

$$\mathcal{L} \supset y_1 \bar{L} \tilde{H} \psi_{1R} + y_2 \bar{\psi}_{1L} \sigma \nu_R + M_1 \bar{\psi}_{1L} \psi_{1R}. \quad (2.1)$$

The existence of these terms is responsible to give tree-level mass to the neutrinos via Dirac seesaw as shown in Fig. 4 (left diagram). It is not difficult to see that the model diagram T1-iii-5-B demands the existence of a fermion $\psi_1 \sim (1, 2, -\frac{1}{2}, -4)$, which allows the following terms in the Lagrangian:

$$\mathcal{L} \supset y'_1 \bar{L} \sigma \psi_{1R} + y'_2 \bar{\psi}_{1L} \tilde{H} \nu_R + M'_1 \bar{\psi}_{1L} \psi_{1R}. \quad (2.2)$$

Hence, also leads to tree-level Dirac seesaw as demonstrated in Fig. 4 (right diagram). Following similar arguments, diagrams T1-iii-5-C and T1-iii-5-D must also be discarded. The same conclusion can be reached for T1-iii-6 diagram as shown in Fig. 2.

2.2 Search for minimal one-loop models without colored particles

From the aforementioned elaborated discussion, we exclude topologies T1-iii,iv,v,vi and in the following build successful minimal models arising from the remaining two topologies,



Figure 4: Tree-level Dirac seesaw reduction from diagrams of type T1-iii-3.

T1-i and T1-ii. Affiliated with topology T1-i, there are three different diagrams corresponding to three different Lorentz structures that we denote by T1-i-1,2,3. Within each of these diagrams, interchanging the two external scalar legs gives two distinct possibilities. Altogether these six possible diagrams are presented in Fig. 5 along with the unique diagram arising from T1-ii topology. Below, we fabricate economical models from these seven diagrams. Quantum numbers of all the particles associated with each of these models are summarized in Table 2.

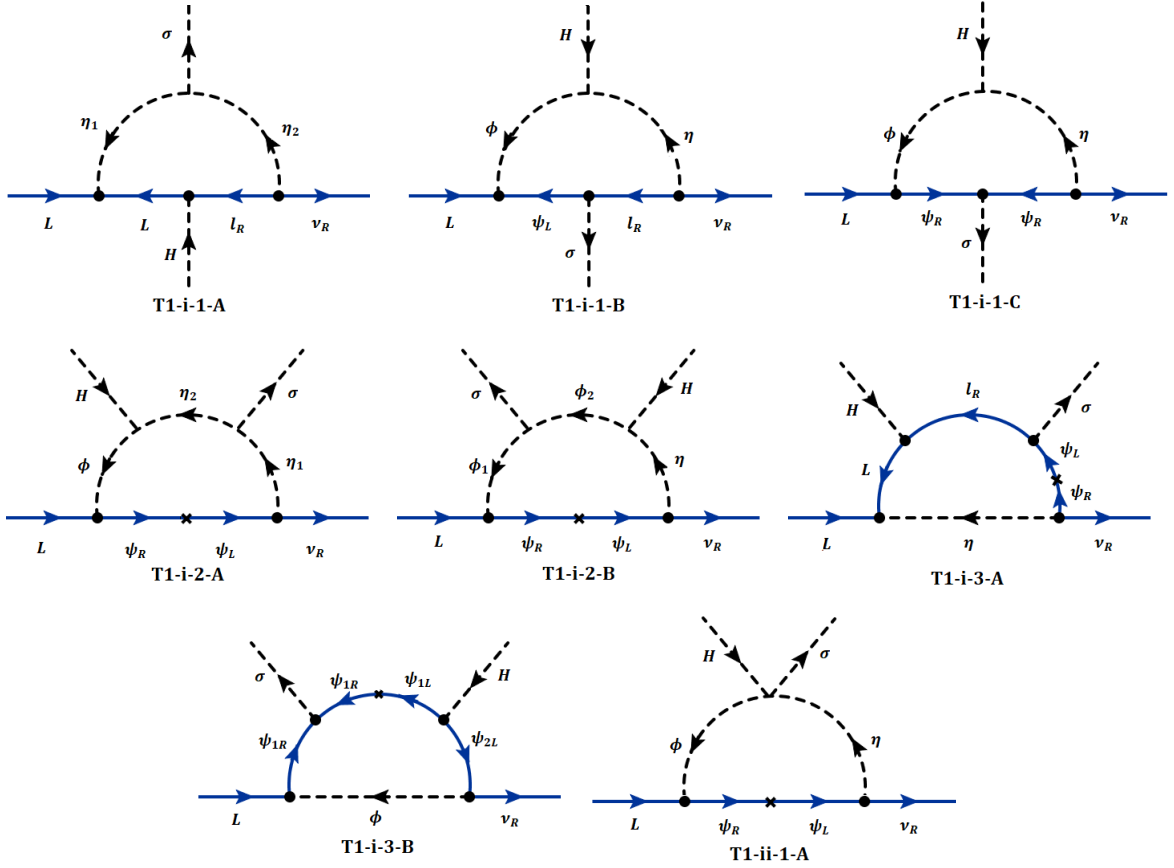


Figure 5: One-loop model diagrams emerging from T1-i and T1-ii topologies in our framework. Quantum numbers associated with each of the models are presented in Table 2. Notation: the color-blind scalars η and ϕ are assumed to be singlet and doublet under $SU(2)_L$.

□ T1-i-1-A:

It is pointed out in Ref. [53] that the most economical model at the one-loop for Dirac neutrino mass in the framework we are working is associated with the T1-i-1-A model diagram. This minimal model consists of only two additional singly charged scalars that are iso-singlets and carry non-zero $B - L$ charges: $\eta_1(1, 1, 1, 2)$ and $\eta_2(1, 1, 1, 5)$. One of the main reasons T1-i-1-A is the simplest among the rest of the one-loop models is, neither any exotic fermion beyond the SM nor any scalar charged under $SU(2)_L$ needs to be introduced.

□ T1-i-1-B/C:

The difference between the T1-i-1-A and T1-i-1-B/C model diagrams is just the swapping of the H and σ scalars. Since, σ is now attached to the internal fermion line instead of the scalar line, more possibilities open up. The most economical models that can be built out of these, require a pair of vector-like Dirac fermions $\psi_{L,R} \sim (1, 1, Y, \alpha)$ in addition to two scalars. In T1-i-1-B model diagram, since one of the internal fermions is ℓ_R , one requires $Y = -1$ and $\alpha = -4$. As a result, one of the BSM scalars must be a singly charged state and the other an iso-doublet with $3/2$ hypercharge. However, it should be kept in mind that such a model (T1-i-1-B) is somewhat phenomenologically constrained. The reason is, it requires the fermionic state $\psi_{L,R} \sim (1, 1, -1, -4)$ and contains the following terms in the Lagrangian:

$$\mathcal{L} \supset \begin{pmatrix} \bar{L} & \overline{\psi_L} \end{pmatrix} \begin{pmatrix} y_e H & y \sigma \\ y' \sigma^* & M_\psi \end{pmatrix} \begin{pmatrix} \ell_R \\ \psi_R \end{pmatrix}. \quad (2.3)$$

When $U(1)_{B-L}$ and EW symmetries are broken, these terms lead to 6×6 mass matrix for the SM leptons and the vector-like leptons. The mixing among these fields must be small to satisfy all the collider constraints provided that ψ has mass $\sim \mathcal{O}(\text{TeV})$, which requires the off-diagonal Yukawa couplings y, y' to be small in Eq. (2.3).

On the other hand, if only the BSM fermion is inside the loop, then the vertex $\psi_R \psi_R \sigma^*$ associated with the model diagram T1-i-1-C demands $Y = 0$ and $\alpha = 3/2$. Consequently, one of the BSM Higgs is SM singlet and the second one is SM like Higgs doublet with non-zero $B - L$ charge. Quantum numbers corresponding to T1-i-1-B/C model diagrams are written down in Table 2 and the associated Feynman diagrams are presented in Fig. 5.

□ T1-i-2-A/B:

The minimal models that are built from T1-i-2-A and T1-i-2-B both require extension by one pair of fermions $\psi_{L,R}(1, 1, Y, \alpha)$ along with three scalars. The corresponding models presented in Table 2 show that among the three scalars, the former model contains two singlets and one iso-doublet, whereas, the latter model consists of two iso-doublets and a singlet, all carrying non-zero $B - L$ charge. Note that for T1-i-2-A and T1-i-2-B model diagrams, if $Y = 0$ then $\alpha \neq -1$ must be realized, otherwise they lead to tree-level Dirac seesaw to generate neutrino mass. Also to avoid direct tree-level mass term for the case of T1-i-2-A (T1-i-2-B), if $Y = -1$ or $Y = 0$ then $\alpha \neq -7, -5, 2, 5$ ($\alpha \neq -10, -7, -1, 2$) must be satisfied to forbid the induced VEV of the multiplet ϕ .

Diagram	Models	New Fields		Relevant terms in Lagrangian	New ?
		Scalars	Fermions		
T1-i-1	T1-i-1-A	$\eta_1(1, 1, 1, 2)$ $\eta_2(1, 1, 1, 5)$	—	$y_1 \overline{L^c} \epsilon \eta_1 L + y_e \overline{L} H l_R$ $+ y_2 \overline{l_R^c} \eta_2 \nu_R + \mu \eta_2 \eta_1^* \sigma^*$	[49, 53]
	T1-i-1-B	$\eta(1, 1, 1, 5)$ $\phi(1, 2, \frac{3}{2}, 5)$	$\psi_{L,R}(1, 1, -1, -4)$	$y_1 \overline{L^c} \epsilon \phi \psi_L + y_2 \overline{\psi_L} \sigma^* l_R$ $+ y_3 \overline{l_R^c} \eta \nu_R + \mu \phi^* H \eta$	✓
	T1-i-1-C	$\eta(1, 1, 0, \frac{5}{2})$ $\phi(1, 2, \frac{1}{2}, \frac{5}{2})$	$\psi_{L,R}(1, 1, 0, \frac{3}{2})$	$y_1 \overline{L} \epsilon \phi^* \psi_R + y_2 \overline{\psi_R^c} \sigma^* \psi_R$ $+ y_3 \overline{\psi_R^c} \eta \nu_R + \mu \phi^* H \eta$	✓
T1-i-2	T1-i-2-A	$\eta_1(1, 1, Y, 4 + \alpha)$ $\eta_2(1, 1, Y, 1 + \alpha)$ $\phi(1, 2, Y + \frac{1}{2}, 1 + \alpha)$	$\psi_{L,R}(1, 1, Y, \alpha)$	$M_\psi \overline{\psi_L} \psi_R + y_1 \overline{L} \epsilon \phi^* \psi_R$ $+ y_2 \overline{\psi_L} \eta_1 \nu_R + \mu_1 \eta_1 \eta_2^* \sigma^*$ $+ \mu_2 \phi^* H \eta_2$	✓
	T1-i-2-B	$\eta(1, 1, Y, 4 + \alpha)$ $\phi_1(1, 2, Y + \frac{1}{2}, 1 + \alpha)$ $\phi_2(1, 2, Y + \frac{1}{2}, 4 + \alpha)$	$\psi_{L,R}(1, 1, Y, \alpha)$	$M_\psi \overline{\psi_L} \psi_R + y_1 \overline{L} \epsilon \phi_1^* \psi_R$ $+ y_2 \overline{\psi_L} \eta \nu_R + \mu_1 H \eta \phi_2^*$ $+ \mu_2 \phi_1^* \phi_2 \sigma^*$	✓
T1-i-3	T1-i-3-A	$\eta(1, 1, 1, 2)$	$\psi_{L,R}(1, 1, -1, 2)$	$M_\psi \overline{\psi_L} \psi_R + y_1 \overline{L^c} \epsilon \eta L$ $+ y_2 \overline{\psi_R^c} \eta \nu_R + y_3 \overline{\psi_L} \sigma l_R$ $+ y_e \overline{L} H l_R$	✓
	T1-i-3-B	$\phi(1, 2, \frac{1}{2}, \frac{5}{2})$	$\psi_{1L,R}(1, 1, 0, \frac{3}{2})$ $\psi_{2L,R}(1, 2, \frac{1}{2}, -\frac{3}{2})$	$M_\psi \overline{\psi_{1L}} \psi_{1R} + y_1 \overline{L} \epsilon \phi^* \psi_{1R}$ $+ y_2 \overline{\psi_{1R}^c} \sigma^* \psi_{1R} + y_3 \overline{\psi_{2L}} \phi \nu_R$ $+ y_4 \overline{\psi_{2L}^c} H^* \psi_{1L}$	✓
T1-ii-1	T1-ii-1-A	$\eta(1, 1, Y, 4 + \alpha)$ $\phi(1, 2, Y + \frac{1}{2}, 1 + \alpha)$	$\psi_{L,R}(1, 1, Y, \alpha)$	$M_\psi \overline{\psi_L} \psi_R + y_1 \overline{L} \epsilon \phi^* \psi_R$ $+ y_2 \overline{\psi_L} \eta \nu_R + \lambda \phi^* H \eta \sigma^*$	[48, 49]

Table 2: Minimal one-loop models without colored particles constructed from $d = 5$ effective operator given in Eq. (1.2). Notation: the color-blind scalars η and ϕ are assumed to be singlet and doublet under $SU(2)_L$. A term of the form $\phi^* H$ in the Lagrangian refers to $\phi^\dagger H$, and furthermore, $\epsilon H^* \equiv \tilde{H}$ and $\epsilon \phi^* \equiv \tilde{\phi}$.

□ T1-i-3-A/B:

To build viable models out of T1-i-3-A one needs a pair of BSM fermions $\psi \sim (1, 1, -1, 2)$ and a singly charged scalar $(1, 1, 1, 2)$. Whereas, this model is very economical, but the viability of the T1-i-3-B model diagram, obtained by flipping H with σ requires two pairs of fermions: an iso-singlet $\psi_1(1, 1, 0, 3/2)$ and an iso-doublet $\psi_2(1, 2, 1/2, -3/2)$ along with a scalar doublet $\phi(1, 2, 1/2, 5/2)$.

□ T1-ii-1-A:

The last in our list for the one-loop models is the one derived from T1-ii topology, which is unique in structure since, interchanging the two external Higgs lines do not lead to different possibilities. The associated model diagram T1-ii-1-A is presented in Fig. 5. The minimal model constructed from this diagram requires an iso-doublet scalar, an iso-singlet scalar and a pair of iso-singlet fermions $\psi \sim (1, 1, Y, \alpha)$ listed in Table 2. Here, to avoid any direct mass term between the left-handed and the right-handed neutrinos, for $Y = -1$, $\alpha \neq 2$ must be realized. Furthermore, to forbid tree-level Dirac seesaw, if $Y = 0$, $\alpha \neq -1$ constraint must be imposed as well.

At this point, it is important to note that any model that is built from diagram T1-i-2 will always lead to a second Feynman diagram which is exactly the same as T1-ii-1, even though these two sets of diagrams originate from completely different topologies. From Fig.

5 one sees that in diagram T1-i-2, removing the scalar that is propagating in between the two scalar cubic vertices immediately gives a second diagram which is the same as T1-i-2. In this sense, unlike the rest of the models presented here, models emerging from T1-i-2-A,B diagrams cannot be considered as genuine and, we refer these two as *non-genuine* model diagrams. Here *non-genuinity* does not refer to one-loop to tree-level reduction.

2.3 Search for minimal one-loop models with colored particles

As discussed in Sec. 1, we also include colored particles in our search. In this section, we build the minimal models with BSM states running in the loop that are charged under $SU(3)_C$. Following the above discussions, here we only consider the topologies that can provide viable models. Whereas it is straightforward to build the associated colored versions of the models, however, for some of the cases, models with and without colored particles differ in structure. Here we very briefly discuss the models and point out the differences when required. Successful minimal model diagrams with colored particles are presented in Fig. 6 and their quantum numbers are listed in Table 3. To distinguish these models, we label the model diagrams by T1-x-y-z(C), here C in the parentheses is put to differentiate models with colored particles, compared to models with color singlets.

□ T1-i-1-A/B/C/D(C):

The model diagram T1-i-1-A(C) is straightforwardly obtained from T1-i-1-A by replacing the two singly charged scalars $\eta_1(1, 1, 1, 2) + \eta_2(1, 1, 1, 5)$ by two scalar leptoquarks $\chi_1(\bar{3}, 1, 1/3, 2/3) + \chi_2(\bar{3}, 1, 1/3, 11/3)$. This choice is uniquely fixed by making the replacements: $L \leftrightarrow Q_L$ and $\ell_R \leftrightarrow d_R$ inside loop in T1-i-1-A to obtain T1-i-1-A(C). Just like T1-i-1-A, this model again can be considered as the most minimal radiative Dirac neutrino mass model with colored particles. Note that a straightforward variation of T1-i-1-A(C), is the interchange $Q_L \leftrightarrow d_R$, which gives rise to the model diagram T1-i-1-B(C). It is worthwhile to mention that no such analogous model with color singlets exists. It is due to fact that $L \leftrightarrow \ell_R$ exchange would give rise to a model which would automatically permit tree-level mass for neutrinos. Even though the model associated to T1-i-1-B(C) also contains only two scalar leptoquarks, but is less economical compared to T1-i-1-A(C) in the sense that both these leptoquarks are in the fundamental representation of $SU(2)_L$. However, both these models are very economical since, no BSM fermionic extension is required.

Two different colored version models can be constructed that are analogous to T1-i-1-B by replacing $\ell_R \leftrightarrow d_R$ (T1-i-1-C(C)) and $\ell_R \leftrightarrow u_R$ (T1-i-1-D(C)) respectively. As noted above, the T1-i-1-B model is phenomenologically somewhat constraining, the same argument follows for T1-i-1-C(C) and T1-i-1-D(C) due to the mixing of the SM fermions with BSM fermionic states. Note however that analogous to T1-i-1-C model diagram with color singlet states, no such colored version model can be constructed with a single pair of BSM fermionic states.

□ T1-i-2-A/B(C), T1-i-3-A/B(C) & T1-ii-1-A(C):

As already pointed out, models fabricated from diagram T1-i-2 are non-genuine and always contain a second diagram which is exactly the same as T1-ii-1 that emerge from a completely different topology and more economical in nature. Allowing color non-singlet states do not alter this fact. Colored version of these models can be straightforwardly built by following the corresponding discussions of the associated models with color singlets.

Whereas the colored extension of T1-i-3-A(C) from T1-i-3-A is straightforward, construction of T1-i-3-B(C) deserves further explanation. As aforementioned, the model built out of T1-i-3-B requires the introduction of two pairs of BSM fermions. It is interesting to note that, the associated colored version, T1-i-3-B(C) is comparatively economical as implementation of this minimal model diagram can be done with just one pair BSM fermions $\psi \sim (3, 1, -1/3, 10/3)$. Besides this fermion, just one more BSM Higgs is employed to complete the loop. For more details on these models see Fig. 6 and Table 3.

Diagram	Models	New Fields		Relevant terms in Lagrangian	New ?
		Scalars	Fermions		
T1-i-1	T1-i-1-A(C)	$\chi_1(\bar{3}, 1, \frac{1}{3}, \frac{2}{3})$ $\chi_2(\bar{3}, 1, \frac{1}{3}, \frac{11}{3})$	—	$y_1 \bar{L}^c \epsilon \chi_1 Q_L + y_d \bar{Q}_L H d_R$ $+ y_2 d_R^c \chi_2 \nu_R + \mu \chi_2 \chi_1^* \sigma^*$	✓
	T1-i-1-B(C)	$\Omega_1(3, 2, \frac{1}{6}, \frac{4}{3})$ $\Omega_2(3, 2, \frac{1}{6}, \frac{13}{3})$	—	$y_1 \bar{d}_R \Omega_1 \epsilon L + y_d \bar{Q}_L H d_R$ $+ y_2 \bar{Q}_L \Omega_2 \nu_R + \mu \Omega_1^* \Omega_2 \sigma^*$	✓
	T1-i-1-C(C)	$\chi(\bar{3}, 1, \frac{1}{3}, \frac{11}{3})$ $\Omega(3, 2, \frac{5}{6}, \frac{11}{3})$	$\psi_{L,R}(3, 1, -\frac{1}{3}, -\frac{8}{3})$	$y_1 \bar{L}^c \epsilon \Omega \psi_L + y_2 \bar{\psi}_L \sigma^* d_R$ $+ y_3 d_R^c \chi \nu_R + \mu \Omega^* H \chi$	✓
	T1-i-1-D(C)	$\chi(\bar{3}, 1, -\frac{2}{3}, \frac{11}{3})$ $\Omega(3, 2, -\frac{1}{6}, \frac{11}{3})$	$\psi_{L,R}(3, 1, \frac{2}{3}, -\frac{8}{3})$	$y_1 \bar{L}^c \epsilon \Omega \psi_L + y_2 \bar{\psi}_L \sigma^* u_R$ $+ y_3 u_R^c \chi \nu_R + \mu \Omega^* H \chi$	✓
T1-i-2	T1-i-2-A(C)	$\chi_1(3, 1, Y, 4 + \alpha)$ $\chi_2(3, 1, Y, 1 + \alpha)$ $\Omega(3, 2, Y + \frac{1}{2}, 1 + \alpha)$	$\psi_{L,R}(3, 1, Y, \alpha)$	$M_\psi \bar{\psi}_L \psi_R + y_1 \bar{L} \epsilon \Omega^* \psi_R$ $+ y_2 \bar{\psi}_L \chi_1 \nu_R + \mu_1 \Omega^* H \chi_2$ $+ \mu_2 \chi_1 \chi_2^* \sigma^*$	✓
	T1-i-2-B(C)	$\chi(3, 1, Y, 4 + \alpha)$ $\Omega_1(3, 2, Y + \frac{1}{2}, 1 + \alpha)$ $\Omega_2(3, 2, Y + \frac{1}{2}, 4 + \alpha)$	$\psi_{L,R}(3, 1, Y, \alpha)$	$M_\psi \bar{\psi}_L \psi_R + y_1 \bar{L} \epsilon \Omega_1^* \psi_R$ $+ y_2 \bar{\psi}_L \chi \nu_R + \mu_1 \Omega_2^* H \chi$ $+ \mu_2 \Omega_1^* \Omega_2 \sigma^*$	✓
T1-i-3	T1-i-3-A(C)	$\chi(\bar{3}, 1, \frac{1}{3}, \frac{2}{3})$	$\psi_{L,R}(3, 1, -\frac{1}{3}, \frac{10}{3})$	$M_\psi \bar{\psi}_L \psi_R + y_1 \bar{L}^c \epsilon \chi Q_L$ $+ y_d \bar{Q}_L H d_R + y_2 \bar{\psi}_R^c \chi \nu_R$ $+ y_3 \bar{\psi}_L \sigma d_R$	✓
	T1-i-3-B(C)	$\Omega(3, 2, \frac{1}{6}, \frac{13}{3})$	$\psi_{L,R}(3, 1, -\frac{1}{3}, \frac{10}{3})$	$M_\psi \bar{\psi}_L \psi_R + y_1 \bar{L} \epsilon \Omega^* \psi_R$ $+ y_d \bar{Q}_L H d_R + y_2 \bar{Q}_L \Omega \nu_R$ $+ y_3 \bar{\psi}_L \sigma d_R$	✓
T1-ii-1	T1-ii-1-A(C)	$\chi(3, 1, Y, 4 + \alpha)$ $\Omega(3, 2, Y + \frac{1}{2}, 1 + \alpha)$	$\psi_{L,R}(3, 1, Y, \alpha)$	$M_\psi \bar{\psi}_L \psi_R + y_1 \bar{L} \epsilon \Omega^* \psi_R$ $+ y_2 \bar{\psi}_L \chi \nu_R + \lambda \Omega^* H \sigma^* \chi$	✓

Table 3: Minimal one-loop models with colored particles constructed from $d = 5$ effective operator given in Eq. (1.2). Notation: the scalars, χ and Ω charged under the color group are assumed to be $SU(2)_L$ singlet and doublet, respectively.

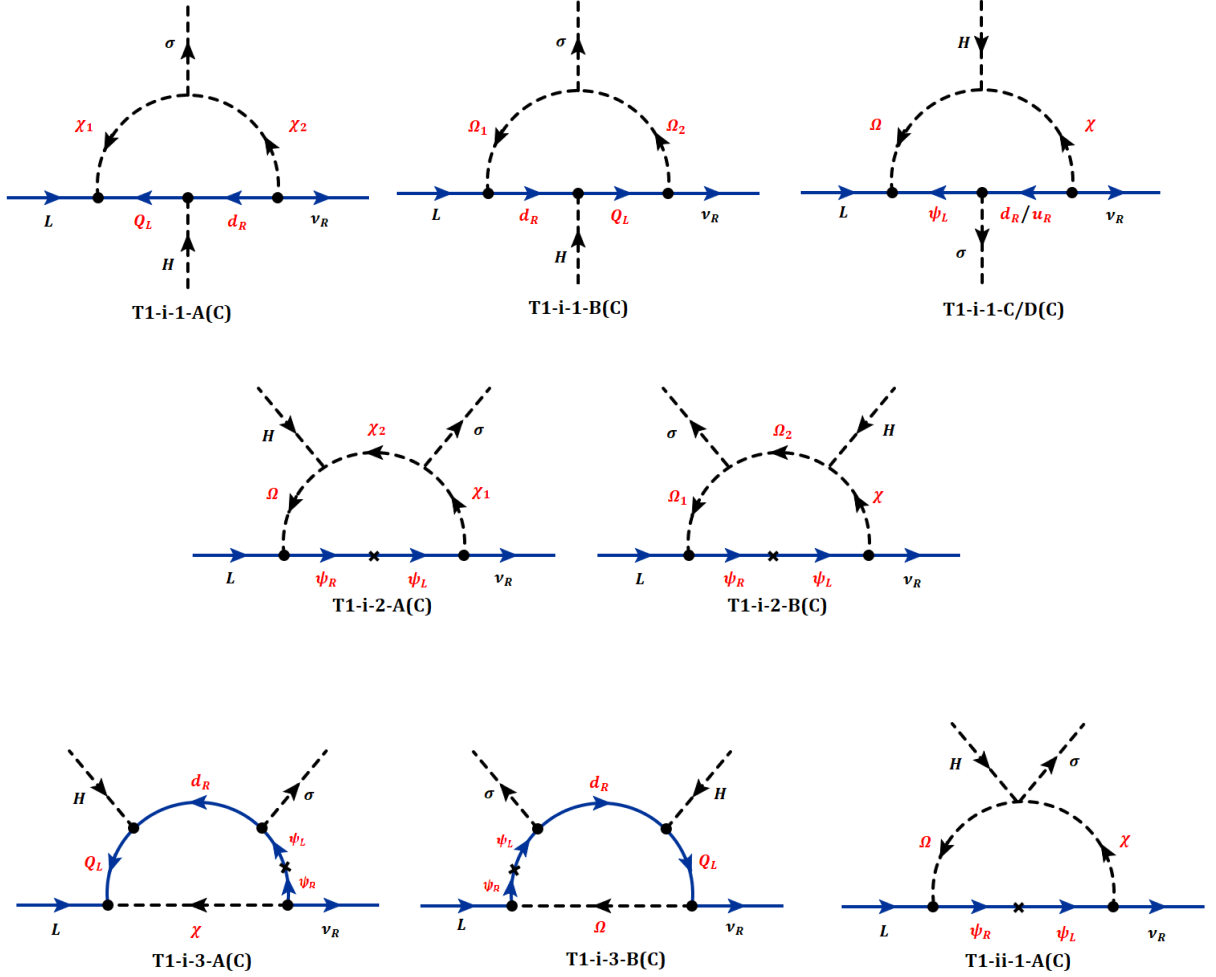


Figure 6: Color version of one loop diagrams emerging from T1-i and T1-ii topologies. Quantum numbers associated with each of the model diagrams are presented in Table 2. Notation: the scalars, χ and Ω charged under the color group are assumed to be $SU(2)_L$ singlet and doublet, respectively.

3 Search for minimal two-loop models

In the previous section, we have systematically built the minimal one-loop Dirac neutrino mass models within our framework. In this section, our goal is to implement a similar methodology to select the minimal two-loop models.

3.1 Generic topologies, nomenclature and selecting viable skeleton diagrams

Following a similar diagrammatic approach as before, all possible two-loop topologies with four external legs can be identified. Excluding the tadpole diagrams, one-particle-reducible two-loop topologies and by removing the topologies involving self-energies in the external legs, in total 29 distinct possibilities are identified in Ref. [79] and for completeness we present them in Fig. 7. In this list, the last 11 of them correspond to non-renormalizable topologies, hence must be discarded immediately.

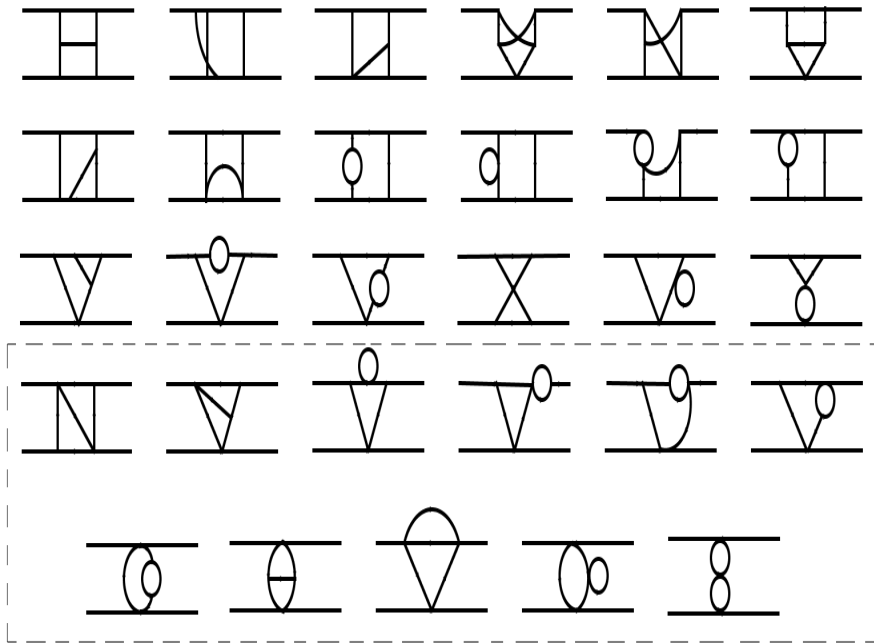


Figure 7: All two-loop topologies arising from $d = 5$ effective operator Eq. (1.2).

While dealing with the remaining 18 two-loop topologies, the number of possible diagrams emerging as a result of specifying the spinors and scalars is quite large compared to the one-loop scenario. Furthermore, when all different swapping of the external legs are also taken into account, a vast number of diagrams appear within our framework because, unlike the Majorana scenario, two of the external fermions are not identical anymore. The same thing is also true for the two external scalar legs, they are not identical. The appearance of the immense number of diagrams is also partly because of the singlet nature of one of the external scalars, which has more freedom to be attached with the internal propagators. In the following, we will demonstrate this by providing explicit examples. Interestingly, all these topologies can be reduced to only six basic diagrams once the external scalar legs are

suppressed [79, 89]. To make our analysis more tractable, instead of starting from each of these 18 possible renormalizable topologies of Fig. 7, we focus on the set of these six basic diagrams derived from the generic two-loop topologies. These are the general diagrams resulting from removing the external scalar legs, and we call them the *skeleton diagrams*, which within our working framework have the structures as shown in Fig. 8. However, each of these skeleton diagrams may lead to quite a few numbers of viable diagrams depending on how the external scalar legs are attached, which makes the analysis of the two-loop models somewhat tedious compared to one-loop case. So the way we proceed is, we start with each of the skeleton diagrams given in Fig. 8, and systematically identify only the most economical model diagram by following our minimality principles as aforementioned. Below we discuss how this filtering process is done at length.

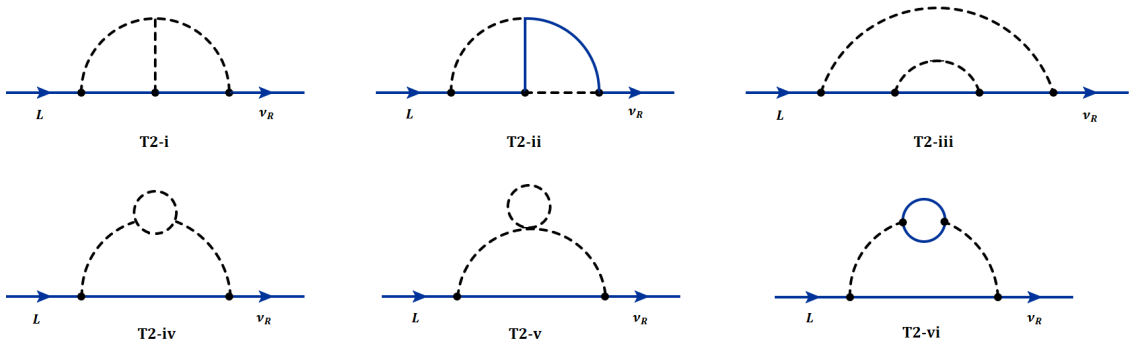


Figure 8: Generic two-loop skeleton diagrams arising from $d = 5$ effective operator Eq. (1.2) from which we build the minimal models. See text for details.

The convention we follow is: each of the skeleton diagrams given in Fig. 8 is labelled with T2-x. Here 2 represents two-loop for obvious reason and $x = i - vi$ to differentiate among the skeleton diagrams from each other. As mentioned above, each of these skeleton diagrams can lead to multiple diagrams after inserting the external scalar legs that we denote by T2-x-y (with $y = 1, 2, 3, \dots$). Furthermore, models that are built from a diagram T2-x-y will be named as T2-x-y-z (where $z = A, B, C, \dots$), that is T2-x-y-z represents a model diagram where the quantum number of all the particles are specified. If the internal particles carry color charge, the model diagram will be named T2-x-y-z(C), here C in the parentheses represents color.

3.2 Search for minimal two-loop models without colored particles

We now proceed to build the associated minimal models from each of the skeleton diagrams.

□ T2-i-y-A:

First, we consider the T2-i skeleton diagram from Fig. 8 and systematically construct all possible diagrams emerging from it and provide our arguments in singling out the most economical model diagram. Note that there are six different ways the SM Higgs doublet

H can be connected with the internal propagators. Furthermore, corresponding to each of these six cases, the scalar singlet, σ can be attached in multiple different ways. By repeating this process for all of these six scenarios, we end up with a total of 43 viable diagrams, T2-i-y ($y=1-43$) as explicitly demonstrated in Fig. 9. In each of these figures, the gray-colored dots represent the different ways of linking σ to the internal propagators. Each of these different possibilities corresponds to a distinct model.

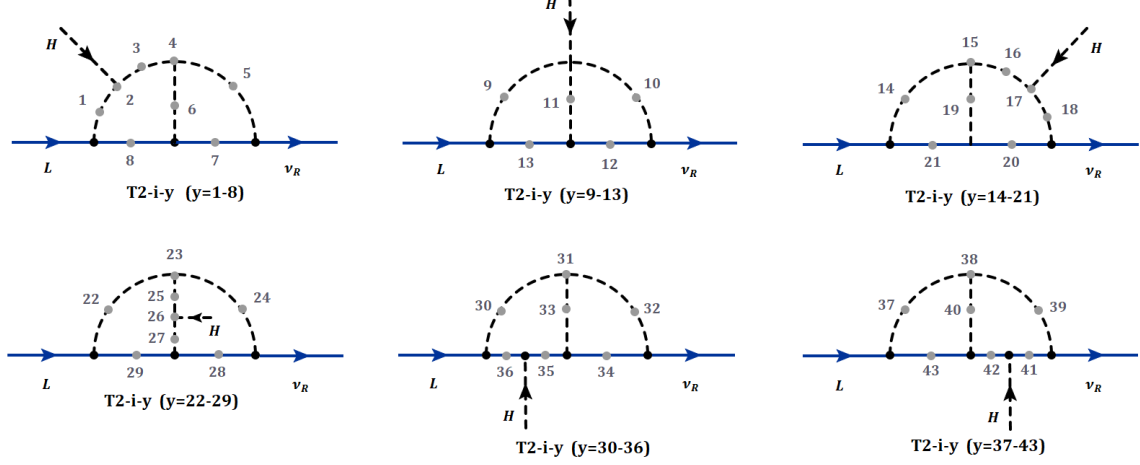


Figure 9: All possible two-loop diagrams manufactured from T2-i skeleton diagram. The gray colored dots represent the different ways of linking σ to the internal propagators, leading to different diagrams T2-i-y, where $y= 1 - 43$.

As aforementioned, we are not going to search for models corresponding to each of these diagrams, rather our focus is to pick the most minimal model diagram originating from T2-i. Going toward this direction, we immediately discard 22 viable diagrams T2-i-y with $y= 7-8, 12-13, 20-21, 28-29, 34-36, 41-43$. The reason is that to build a model from each of these diagrams, requires the introduction of BSM fermions and does not fall into the minimal category. For the rest of the diagrams, in search for finding the minimal model, we fix the internal fermions to be ℓ_R , consequently, 7 of the diagrams T2-i-y with $y= 2-6$ and $10-11$, require a second Higgs doublet (with non-zero $B - L$ charge), rest of the diagrams demand more number of scalar iso-doublets for the completion of the loops, hence do not satisfy our minimality postulates. For these remaining 7 diagrams, we select the models with a minimum number of additional scalars on top of the second iso-doublet, and once this counting is done, we construct the associated explicit model diagrams. Only three of the model diagrams pass our minimality axioms, which are T2-i-2,4,11 and are shown in Fig. 10. Besides the second iso-doublet, the models associated with T2-i-2,4 (T2-i-11) composed of two singly (doubly) charged and a doubly (singly) charged scalars. For the complete quantum numbers of these particles, see Table 4.

From the exercise done above, one can understand that finding the minimal model starting from a certain skeleton diagram can be a bit tedious process. Following the same

procedure for the rest of the skeleton diagrams presented in Fig. 8, we summarize the most economical models in Table 4. In the following, we briefly discuss this systematic analysis in search of the minimal models for the rest of the skeleton diagrams.

□ T2-ii-1/2-A:

Now consider the skeleton diagram T2-ii. Just like the previous example, it is not difficult to see that there are many different ways for the H and σ fields to be attached with the particles running in the loop. Instead of presenting all these possible ways of realizing two-loop neutrino mass models arising from the T2-ii skeleton diagram, we only limit ourselves to the scenario which is the most economical. For the sake of minimality, we choose to insert the SM Higgs doublet in the internal fermion line which is closest to the external L leg. As a result, only BSM iso-singlet representations can be employed to complete the loop diagram, hence satisfies our minimality constraints. Furthermore, to reduce the number of additional scalars, we attach the singlet Higgs σ with one of the internal fermion lines, which however, does not increase the number of required BSM fermion multiplets. The first model (labelled by T2-ii-1-A) we manufacture here is by attaching σ to the fermion propagator that is closest to ν_R external leg. With these choices, one needs two pairs of additional iso-singlet fermions and two BSM iso-singlet scalars to complete the loop diagram. A slight variation of this model can be made (labelled by T2-ii-2-A) by inserting σ in the internal fermion line which is not connected to either of the external fermion legs. The associated model diagrams are presented in Fig. 10 and the quantum numbers of all the needed particles are listed in Table 4.

□ T2-iii-1-A:

To build an economical model from skeleton diagram T2-iii, where different variations of the scalar field insertions are again available, one can follow the arguments that are not very different from the previous models constructed. To aim to find the minimal model, in this particular scenario, we attach the SM Higgs doublet with the internal fermion line⁷ that is closest to the incoming L field. As a result, no BSM scalar doublet needs to be employed in this construction. Furthermore, we connect the external singlet scalar with the inner scalar loop as shown in Fig. 10. This choice of inserting the external scalar fields guarantees the requirement of minimum number of scalar and fermion states, as well as demands only iso-singlet states. Looking at the details of the quantum numbers of the particle contents of this model listed in Table 4, one finds that for $Y = 0$, $\alpha \neq -1$ and $\alpha \neq -7, 4$ must be imposed to avoid tree-level Dirac seesaw and one-loop reduction respectively.

□ T2-iv-1-A:

⁷If instead, H is attached to the outer scalar propagator, completion of the diagram would require one BSM scalar doublet, which can be considered as the next-to-minimal model of similar category, however belong to a different model-diagram.

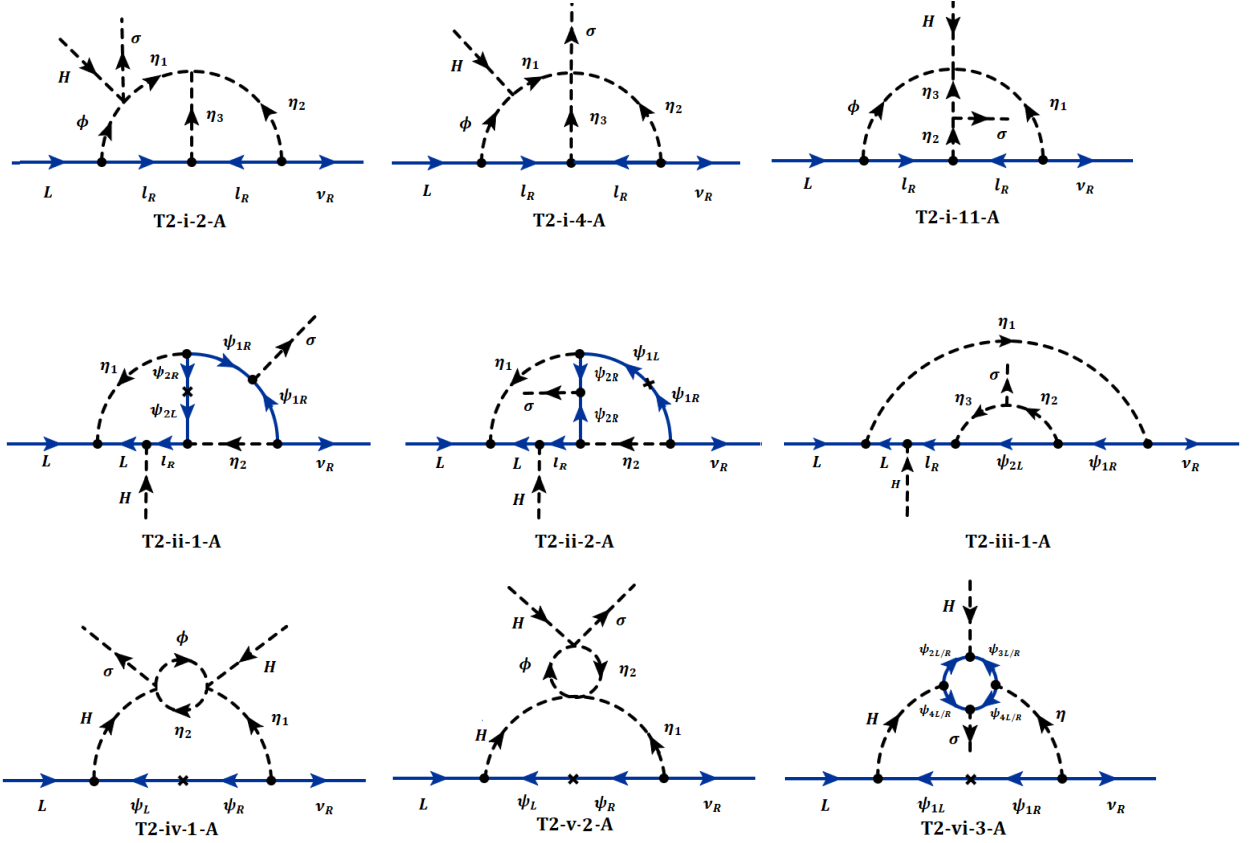


Figure 10: Minimal two-loop model diagrams arising from T2-x ($x=i-vi$) skeleton diagrams. Quantum numbers associated with each of the model diagrams are presented in Table 4. Notation: the color-blind scalars η and ϕ are assumed to be singlet and doublet under $SU(2)_L$.

Here we discuss the skeleton diagram T2-iv. It will be shown that the skeleton diagrams T2-x, with $x=iv-vi$ are very special in nature and share some common features. Building models out of these three cases are very much constraining due to the special nature. First, we discuss the construction of T2-iv in more detail, the analogous arguments can be used to build models from T2-v,vi.

The only viable type of model diagrams that can be formed out of T2-iv must contain the effective scalar vertex of the form $HH\eta$ (with $\eta \sim (1, 1, -1)$ under the SM) as shown in see Fig. 11, here the blob must contain a loop to qualify to be a true two-loop model. The reason for this requirement is, if instead two different Higgs doublets (H and ϕ) are allowed to form this vertex, then the loop contained in the blob immediately reduces to a tree-vertex of the form $H\phi\eta$, hence becomes a one-loop model. On the other hand, if the same SM Higgs is playing the role, then the tree-level vertex automatically vanishes as a result of the antisymmetric property of the term $\mathcal{L} \supset \mu H \epsilon H \eta^-$. Hence, loop to tree-level vertex reduction is not allowed as demonstrated in Fig. 11. With this restriction, still,

there are freedoms to attach the external H with the internal particles contained by the blob. To reduce the number of required additional iso-doublets, we make use of a quartic coupling that consists of external H and internal η with two more BSM scalars as shown in Fig 12-a. Moreover, we have not used the freedom of inserting σ yet, which in fact can be done in four different ways as depicted in Fig. 12-a, T2-iv-y, with $y=1-4$. Out of these four choices, $y=1$ certainly requires the minimum number of additional scalars which is just two. Consequently, we only consider this economical choice and discard the rest of the possibilities. Between these two scalars, one of them is an iso-doublet with non-zero $B-L$ charge $\phi \sim (1, 2, Y, \alpha)$. Note that as aforementioned, if $Y = -1/2$, $\alpha \neq 3$ must be realized to forbid direct mass term for neutrinos at the tree-level. In addition to the scalars, these models require a pair of vector-like Dirac fermions having similar quantum numbers as the e^c under the SM, hence these fermions need to have a mass of order $\mathcal{O}(\text{TeV})$ or higher to be consistent with phenomenological observation as mentioned above.

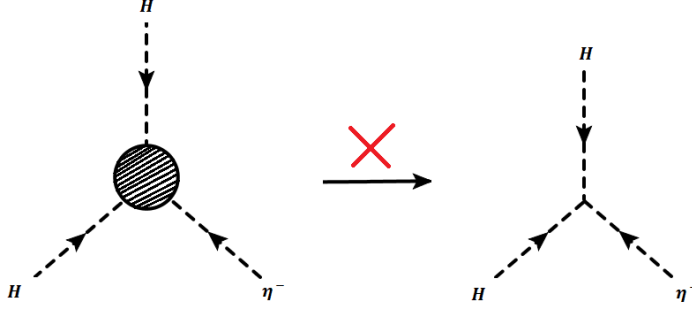


Figure 11: Required type of the internal scalar vertex correction for skeleton diagrams of type T2-iv, T2-v and T2-vi.

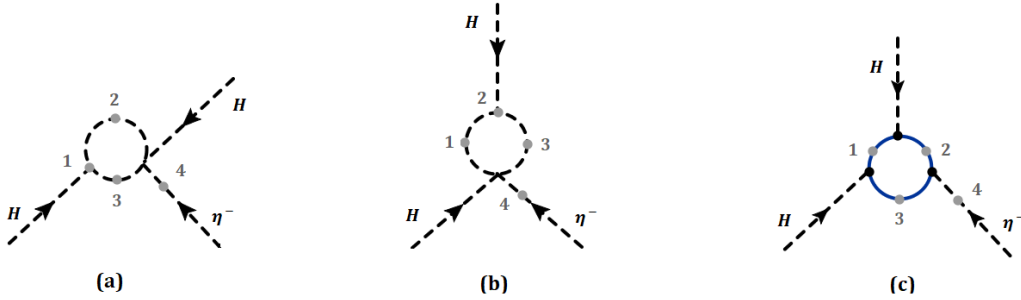


Figure 12: Possible ways of inserting σ field for skeleton diagrams of type T2-iv, T2-v and T2-vi. See text for details.

□ T2-v-1-A:

The above arguments can be repeated for fabricating models from the T2-v skeleton diagram. Even though for this scenario, there is no freedom in inserting external H leg, however, a limited number of freedom is still available associated with σ , which are

demonstrated in Fig. 12-b. Out of these four scenarios, we pick T2-v-2 to build the most economical model which is presented in Fig. 10 and the quantum numbers of all the needed particles are listed in Table 4.

□ T2-vi-3-A:

The last in our list is the T2-vi skeleton diagram, which requires quite a few BSM fermions to complete the loop diagram. Unlike T2-iv, no such quartic scalar vertex is allowed here, hence there is no freedom in connecting H . Though, there are four different ways one can attach σ as depicted in Fig. 12-c, minimality corresponds to T2-vi-3 realization. This choice requires four BM fermions and a singly charged scalar, for details see Table 4.

Even though T2-x (x=iv-vi) diagrams appear to provide divergent loop integrals, but it is not the case. The reason is, when the term $H\epsilon H$ is broken down to its component fields, two same terms emerge with opposite sign, removing the divergences from the difference diagrams resulting in finite neutrino mass, for details see Ref. [79]. Consequently, models arising from T2-iv,v,vi are very special in nature.

Skeleton	Models	New Fields		Relevant terms in Lagrangian	New ?
		Scalars	Fermions		
T2-i	T2-i-2-A	$\eta_1(1, 1, 1, -3)$ $\eta_2(1, 1, 1, 5)$ $\eta_3(1, 1, -2, -2)$ $\phi(1, 2, \frac{1}{2}, 0)$	—	$y_1 \overline{L} \phi l_R + y_2 \overline{l_R^c} \eta_3^* l_R$ $+ y_3 \overline{l_R^c} \eta_2 \nu_R + \mu \eta_1 \eta_2 \eta_3$ $+ \lambda \phi \epsilon H \sigma^* \eta_1^*$	[53]
	T2-i-4-A	$\eta_1(1, 1, 1, 0)$ $\eta_2(1, 1, 1, 5)$ $\eta_3(1, 1, -2, -2)$ $\phi(1, 2, \frac{1}{2}, 0)$	—	$y_1 \overline{L} \phi l_R + y_2 \overline{l_R^c} \eta_3^* l_R$ $+ y_3 \overline{l_R^c} \eta_2 \nu_R + \mu \phi \epsilon H \eta_1^*$ $+ \lambda \eta_1 \eta_2 \eta_3 \sigma^*$	✓
	T2-i-11-A	$\eta_1(1, 1, 1, 5)$ $\eta_2(1, 1, -2, -2)$ $\eta_3(1, 1, -2, -5)$ $\phi(1, 2, \frac{1}{2}, 0)$	—	$y_1 \overline{L} \phi l_R + y_2 \overline{l_R^c} \eta_2^* l_R$ $+ y_3 \overline{l_R^c} \eta_1 \nu_R + \mu \eta_2 \eta_3^* \sigma^*$ $+ \lambda \phi \epsilon H \eta_1 \eta_3$	✓
T2-ii	T2-ii-1-A	$\eta_1(1, 1, 1, 2)$ $\eta_2(1, 1, 0, \frac{5}{2})$	$\psi_{1L,R}(1, 1, 0, \frac{3}{2})$ $\psi_{2L,R}(1, 1, -1, -\frac{7}{2})$	$M_{\psi_2} \overline{\psi_{2L}} \psi_{2R} + y_1 \overline{L^c} \epsilon \eta_1 L$ $+ y_2 \overline{\psi_{2L}} \eta_2^* l_R + y_3 \overline{\psi_{1R}^c} \eta_2 \nu_R$ $+ y_4 \overline{\psi_{1R}^c} \eta_1 \psi_{2R} + y_5 \overline{\psi_{1R}^c} \sigma^* \psi_{1R}$ $+ y_e \overline{L} H l_R$	✓
	T2-ii-2-A	$\eta_1(1, 1, 1, 2)$ $\eta_2(1, 1, -1, \frac{1}{2})$	$\psi_{1L,R}(1, 1, 1, \frac{7}{2})$ $\psi_{2L,R}(1, 1, 0, \frac{3}{2})$	$M_{\psi_1} \overline{\psi_{1L}} \psi_{1R} + y_1 \overline{L^c} \epsilon \eta_1 L$ $+ y_2 \overline{\psi_{2R}^c} \eta_2^* l_R + y_3 \overline{\psi_{1R}^c} \eta_2 \nu_R$ $+ y_4 \overline{\psi_{1L}} \eta_1 \psi_{2R} + y_5 \overline{\psi_{2R}^c} \sigma^* \psi_{2R}$ $+ y_e \overline{L} H l_R$	✓
T2-iii	T2-iii-1-A	$\eta_1(1, 1, -1, -2)$ $\eta_2(1, 1, -(Y+1), 2-\alpha)$ $\eta_3(1, 1, -(Y+1), -(1+\alpha))$	$\psi_{1L,R}(1, 1, -1, 2)$ $\psi_{2L,R}(1, 1, Y, \alpha)$	$y_1 \overline{L^c} \eta_1^* L + y_2 \overline{\psi_{2L}} \eta_3^* l_R$ $+ y_3 \overline{\psi_{2L}} \eta_2^* \psi_{1R} + y_4 \overline{\psi_{1R}^c} \eta_1^* \nu_R$ $+ y_e \overline{L} H l_R + \mu \eta_2 \eta_3^* \sigma^*$	✓
T2-iv	T2-iv-1-A	$\eta_1(1, 1, -1, 3)$ $\eta_2(1, 1, Y - \frac{1}{2}, \alpha + 3)$ $\phi(1, 2, Y, \alpha)$	$\psi_{L,R}(1, 1, 1, 1)$	$M_{\psi} \overline{\psi_L} \psi_R + y_1 \overline{L^c} H^* \psi_L$ $+ y_2 \overline{\psi_R^c} \eta_1 \nu_R + \lambda_1 \phi^* H \sigma^* \eta_2$ $+ \lambda_2 \phi \epsilon H \eta_1 \eta_2^*$	✓
T2-v	T2-v-2-A	$\eta_1(1, 1, -1, 3)$ $\eta_2(1, 1, Y + \frac{1}{2}, \alpha - 3)$ $\phi(1, 2, Y, \alpha)$	$\psi_{L,R}(1, 1, 1, 1)$	$M_{\psi} \overline{\psi_L} \psi_R + y_1 \overline{L^c} H^* \psi_L$ $+ y_2 \overline{\psi_R^c} \eta_1 \nu_R + \lambda_1 \phi^* H \eta_1 \eta_2$ $+ \lambda_2 \phi \epsilon H \sigma^* \eta_2^*$	✓
T2-vi	T2-vi-3-A	$\eta(1, 1, -1, 3)$	$\psi_{1L,R}(1, 1, 1, 1)$ $\psi_{2L,R}(1, 2, \frac{1}{2}, -\frac{3}{2})$ $\psi_{3L,R}(1, 1, -1, \frac{3}{2})$ $\psi_{4L,R}(1, 1, 0, \frac{3}{2})$	$M_{\psi_1} \overline{\psi_{1L}} \psi_{1R} + y_1 \overline{L^c} H^* \psi_{1L}$ $+ y_2 \overline{\psi_{1R}^c} \eta \nu_R$ $+ y_3 \overline{\psi_{4L/R}^c} \psi_{4L/R} \sigma^*$ $+ y_4 \overline{\psi_{2L/R}^c} \psi_{4L/R} H^*$ $+ y_5 \overline{\psi_{2L/R}^c} \psi_{3L/R} \epsilon H$ $+ y_6 \overline{\psi_{3L/R}^c} \psi_{4L/R} \eta^*$	✓

Table 4: Minimal two-loop models without colored particles constructed from $d = 5$ effective operator given in Eq. (1.2). Notation: the color-blind scalars η and ϕ are assumed to be singlet and doublet under $SU(2)_L$.

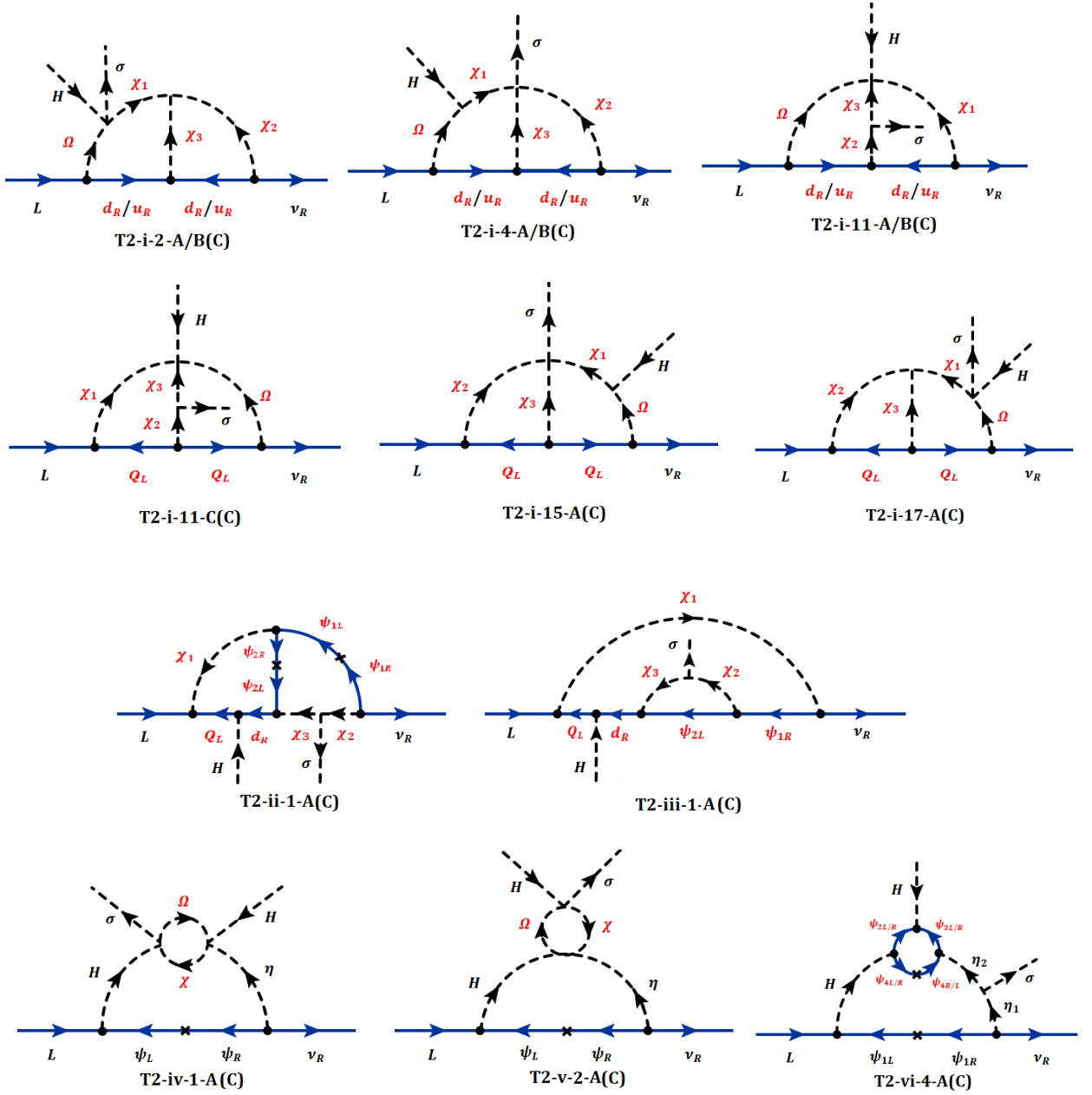


Figure 13: Color version of the minimal two-loop model diagrams arising from T-II-1,2,3,4,5 skeleton diagrams. Quantum numbers associated with each of the model diagrams are presented in Table 5. Notation: the color-blind scalars η and ϕ are assumed to be singlet and doublet under $SU(2)_L$. The scalars, χ and Ω charged under the color group are assumed to be $SU(2)_L$ singlet and doublet, respectively.

Skeleton	Models	New Fields		Relevant terms in Lagrangian	New ?
		Scalars	Fermions		
T2-i	T2-i-2-A(C)	$\chi_1(\bar{3}, 1, \frac{1}{3}, -\frac{13}{3})$ $\chi_2(\bar{3}, 1, \frac{1}{3}, \frac{11}{3})$ $\chi_3(\bar{3}, 1, -\frac{2}{3}, \frac{2}{3})$ $\Omega(\bar{3}, 2, -\frac{1}{6}, -\frac{4}{3})$	—	$y_1 \bar{L} \Omega d_R + y_2 \bar{d}_R^c \chi_3^* d_R$ $+ y_3 \bar{d}_R^c \chi_2 \nu_R + \mu \chi_1 \chi_2 \chi_3$ $+ \lambda \Omega \epsilon H \sigma^* \chi_1^*$	✓
	T2-i-2-B(C)	$\chi_1(\bar{3}, 1, -\frac{2}{3}, -\frac{13}{3})$ $\chi_2(\bar{3}, 1, -\frac{2}{3}, \frac{11}{3})$ $\chi_3(\bar{3}, 1, \frac{4}{3}, \frac{2}{3})$ $\Omega(\bar{3}, 2, -\frac{7}{6}, -\frac{4}{3})$	—	$y_1 \bar{L} \Omega u_R + y_2 \bar{u}_R^c \chi_3^* u_R$ $+ y_3 \bar{u}_R^c \chi_2 \nu_R + \mu \chi_1 \chi_2 \chi_3$ $+ \lambda \Omega \epsilon H \sigma^* \chi_1^*$	✓
	T2-i-4-A(C)	$\chi_1(\bar{3}, 1, \frac{1}{3}, -\frac{4}{3})$ $\chi_2(\bar{3}, 1, \frac{1}{3}, \frac{11}{3})$ $\chi_3(\bar{3}, 1, -\frac{2}{3}, \frac{2}{3})$ $\Omega(\bar{3}, 2, -\frac{1}{6}, -\frac{4}{3})$	—	$y_1 \bar{L} \Omega d_R + y_2 \bar{d}_R^c \chi_3^* d_R$ $+ y_3 \bar{d}_R^c \chi_2 \nu_R + \mu \Omega \epsilon H \chi_1^*$ $+ \lambda \chi_1 \chi_2 \chi_3 \sigma^*$	✓
	T2-i-4-B(C)	$\chi_1(\bar{3}, 1, -\frac{2}{3}, -\frac{4}{3})$ $\chi_2(\bar{3}, 1, -\frac{2}{3}, \frac{11}{3})$ $\chi_3(\bar{3}, 1, \frac{4}{3}, \frac{2}{3})$ $\Omega(\bar{3}, 2, -\frac{7}{6}, -\frac{4}{3})$	—	$y_1 \bar{L} \Omega u_R + y_2 \bar{u}_R^c \chi_3^* u_R$ $+ y_3 \bar{u}_R^c \chi_2 \nu_R + \mu \Omega \epsilon H \chi_1^*$ $+ \lambda \chi_1 \chi_2 \chi_3 \sigma^*$	✓
	T2-i-11-A(C)	$\chi_1(\bar{3}, 1, \frac{1}{3}, \frac{11}{3})$ $\chi_2(\bar{3}, 1, -\frac{2}{3}, \frac{2}{3})$ $\chi_3(\bar{3}, 1, -\frac{2}{3}, -\frac{7}{3})$ $\Omega(\bar{3}, 2, -\frac{1}{6}, -\frac{4}{3})$	—	$y_1 \bar{L} \Omega d_R + y_2 \bar{d}_R^c \chi_3^* d_R$ $+ y_3 \bar{d}_R^c \chi_1 \nu_R + \mu \chi_2 \chi_3^* \sigma^*$ $+ \lambda \Omega \epsilon H \chi_1 \chi_3$	✓
	T2-i-11-B(C)	$\chi_1(\bar{3}, 1, -\frac{2}{3}, \frac{11}{3})$ $\chi_2(\bar{3}, 1, \frac{4}{3}, \frac{2}{3})$ $\chi_3(\bar{3}, 1, \frac{4}{3}, -\frac{7}{3})$ $\Omega(\bar{3}, 2, -\frac{7}{6}, -\frac{4}{3})$	—	$y_1 \bar{L} \Omega u_R + y_2 \bar{u}_R^c \chi_2^* u_R$ $+ y_3 \bar{u}_R^c \chi_1 \nu_R + \mu \chi_2 \chi_3^* \sigma^*$ $+ \lambda \Omega \epsilon H \chi_1 \chi_3$	✓
	T2-i-11-C(C)	$\chi_1(3, 1, -\frac{1}{3}, -\frac{2}{3})$ $\chi_2(3, 1, -\frac{1}{3}, \frac{7}{3})$ $\chi_3(3, 1, -\frac{1}{3}, -\frac{11}{3})$ $\Omega(3, 2, \frac{1}{6}, \frac{13}{3})$	—	$y_1 \bar{L}^c \chi_1^* Q_L + y_2 \bar{Q}_L^c \epsilon Q_L \chi_2$ $+ y_3 \bar{Q}_L \Omega \nu_R + \mu \chi_2 \chi_3^* \sigma^*$ $+ \lambda \Omega \epsilon H \chi_1 \chi_3$	✓
	T2-i-15-A(C)	$\chi_1(3, 1, \frac{2}{3}, \frac{13}{3})$ $\chi_2(3, 1, -\frac{1}{3}, \frac{2}{3})$ $\chi_3(3, 1, -\frac{1}{3}, -\frac{2}{3})$ $\Omega(3, 2, \frac{1}{6}, \frac{13}{3})$	—	$y_1 \bar{L}^c \epsilon \chi_2^* Q_L + y_2 \bar{Q}_L^c \epsilon Q_L \chi_3$ $+ y_3 \bar{Q}_L \Omega \nu_R + \mu \chi_1^* \Omega \epsilon H$ $+ \lambda \chi_1 \chi_2 \chi_3 \sigma^*$	✓
	T2-i-17-A(C)	$\chi_1(3, 1, \frac{2}{3}, \frac{4}{3})$ $\chi_2(3, 1, -\frac{1}{3}, -\frac{2}{3})$ $\chi_3(3, 1, -\frac{1}{3}, -\frac{2}{3})$ $\Omega(3, 2, \frac{1}{6}, \frac{13}{3})$	—	$y_1 \bar{L}^c \epsilon \chi_2^* Q_L + y_2 \bar{Q}_L^c \epsilon Q_L \chi_3$ $+ y_3 \bar{Q}_L \Omega \nu_R + \mu \chi_1 \chi_2 \chi_3$ $+ \lambda \sigma^* \chi_1^* \Omega \epsilon H$	✓
T2-ii	T2-ii-1-A(C)	$\chi_1(\bar{3}, 1, \frac{1}{3}, \frac{2}{3})$ $\chi_2(\bar{3}, 1, -Y - \frac{1}{3}, \frac{10}{3} - \alpha)$ $\chi_3(\bar{3}, 1, -Y - \frac{1}{3}, \frac{1}{3} - \alpha)$	$\psi_{1L,R}(3, 1, Y + \frac{1}{3}, \alpha + \frac{2}{3})$ $\psi_{2L,R}(\bar{3}, 1, Y, \alpha)$	$M_{\psi_1} \bar{\psi}_{1L} \psi_{1R} + M_{\psi_2} \bar{\psi}_{2L} \psi_{2R}$ $+ y_1 \bar{L}^c \epsilon \chi_1 Q_L + y_2 \bar{\psi}_{2L} \chi_3^* d_R$ $+ y_3 \bar{\psi}_{1R}^c \chi_2 \nu_R + y_4 \bar{\psi}_{1L} \chi_1 \psi_{2R}$ $+ y_d \bar{Q}_L H d_R + \mu \chi_2 \chi_3^* \sigma^*$	✓
T2-iii	T2-iii-1-A(C)	$\chi_1(3, 1, -\frac{1}{3}, \frac{2}{3})$ $\chi_2(\bar{3}, 1, -(Y + \frac{1}{3}), \frac{10}{3} - \alpha)$ $\chi_3(\bar{3}, 1, -(Y + \frac{1}{3}), \frac{1}{3} - \alpha)$	$\psi_{1L,R}(3, 1, -\frac{1}{3}, \frac{10}{3})$ $\psi_{2L,R}(\bar{3}, 1, Y, \alpha)$	$y_1 \bar{Q}_L^c \chi_1^* L + y_2 \bar{\psi}_{2L} \chi_3^* d_R$ $+ y_3 \bar{\psi}_{2L} \chi_2^* \psi_{1R} + y_4 \bar{\psi}_{1R}^c \chi_1^* \nu_R$ $+ y_d \bar{Q}_L H d_R + \mu \chi_2 \chi_3^* \sigma^*$	✓
T2-iv	T2-iv-1-A(C)	$\eta(1, 1, -1, 3)$ $\chi(3, 1, Y - \frac{1}{2}, \alpha + 3)$ $\Omega(3, 2, Y, \alpha)$	$\psi_{L,R}(1, 1, 1, 1)$	$M_{\psi} \bar{\psi}_L \psi_R + y_1 \bar{L}^c H^* \psi_L$ $+ y_2 \bar{\psi}_R^c \eta \nu_R + \lambda_1 \Omega^* H \sigma^* \chi$ $+ \lambda_2 \Omega \epsilon H \eta \chi^*$	✓
T2-v	T2-v-2-A(C)	$\eta_1(1, 1, -1, 3)$ $\chi(3, 1, Y + \frac{1}{2}, \alpha - 3)$ $\Omega(3, 2, Y, \alpha)$	$\psi_{L,R}(1, 1, 1, 1)$	$M_{\psi} \bar{\psi}_L \psi_R + y_1 \bar{L}^c H^* \psi_L$ $+ y_2 \bar{\psi}_R^c \eta \nu_R + \lambda_1 \Omega^* H \eta \chi$ $+ \lambda_2 \Omega \epsilon H \sigma^* \chi^*$	✓
T2-vi	T2-vi-4-A(C)	$\eta_1(1, 1, -1, 3)$ $\eta_2(1, 1, -1, 0)$	$\psi_{1L,R}(1, 1, 1, 1)$ $\psi_{2L,R}(3, 2, Y, \alpha)$ $\psi_{3L,R}(\bar{3}, 1, -Y - \frac{1}{2}, -\alpha)$ $\psi_{4L,R}(\bar{3}, 1, -Y + \frac{1}{2}, -\alpha)$	$M_{\psi_1} \bar{\psi}_{1L} \psi_{1R} + M_{\psi_4} \bar{\psi}_{4L} \psi_{4R}$ $+ y_1 \bar{L}^c H^* \psi_{1L} + y_2 \bar{\psi}_{1R}^c \eta_1 \nu_R$ $+ y_3 \bar{\psi}_{2L}^c \psi_{3L} \psi_{4L/R} H^*$ $+ y_4 \bar{\psi}_{2L}^c \psi_{3L} \psi_{4L/R} \epsilon H$ $+ y_5 \bar{\psi}_{4R} \psi_{3L/R} \eta_2^* + \mu \eta_1 \eta_2^* \sigma^*$	✓

Table 5: Minimal two-loop models with colored particles constructed from $d = 5$ effective operator given in Eq. (1.2). Each of the models contains $\sigma(1, 1, 0, 3)$ that breaks the $U(1)_{B-L}$ symmetry. Notation: the color-blind scalars η and ϕ are assumed to be singlet and doublet under $SU(2)_L$. The scalars, χ and Ω charged under the color group are assumed to be $SU(2)_L$ singlet and doublet, respectively.

3.3 Search for minimal two-loop models with colored particles

In this section, we carry out our search for finding minimal two-loop models from various topologies introduced above by employing colored particles in the internal lines.

□ T2-i-y-A/B/C(C):

We start with the T2-i skeleton diagram as shown in Fig. 8. As already explained above, this leads to 43 diagrams T2-i-y ($y=1-43$) presented in Fig. 9, out of which, we have identified 3 minimal candidate models for the scenario with color singlet states. The case with colored particles running in the loops is somewhat different and without introducing any new fermions, we find 9 candidates. Two such cases are built out of T2-i-2 diagram, where the internal fermions are either d_R or u_R (which are labelled as T2-i-A(C) and T2-i-2-B(C)). The same thing can be repeated for both T2-i-4 and T2-i-11, resulting in another 4 more minimal models (labelled as T2-i-4-A/B(C) and T2-i-11-A/B(C)). On the contrary, when the internal fermion line is taken to be Q_L instead of either d_R or u_R , in addition to T2-i-11, two more different models can be fabricated out of T2-i-15 and T2-i-17 diagrams that also do not require any fermions BSM. All these 9 different models are presented in Fig. 13 and their particle contents are summarized in Table 4. Note that in these models, the scalars carrying colors are triplets (or anti-triplets), which is in fact, the lowest dimensional representation under $SU(3)_C$.

One can immediately construct variations of these models by replacing the color anti-triplet χ_3 in T2-i-y-z(C) ($y=2,4,11$, $z=A,B$) and the color anti-triplet χ_2 in T2-i-y-z(C) ($y=11$, $z=A,B$) by $SU(3)_C$ sextets (since for $SU(3)$ group, $\bar{3} \times \bar{3} \supset \bar{6}$ and $6 \times \bar{6} \supset 1$), which however are not listed in Table 5 due to our minimality arguments. Similar variation can be done for T2-i-11-C(C) by replacing the color triplets $\chi_{2,3}$ by color sextets and in T2-i-y-z(C) (with $y=15,17$ and $z=A$) by replacing the color triplet χ_3 by a color sextet.

□ T2-ii-1-A(C) & T2-iii-1-A(C):

Colored extension of models arising from T2-ii and T2-iii skeleton diagrams can be done straightforwardly following the discussions presented above for models with color singlet states. To do so, L and ℓ_R in T2-ii-1-A are replaced by Q_L and d_R that results in T2-ii-1-A(C) model diagram. Subsequently, the rest of the internal particles must carry color (color triplets or anti-triplets). Similarly, in T2-iii-1-A, $L \leftrightarrow Q_L$ and $\ell_R \leftrightarrow d_R$ replacements are made in the internal fermion line adjacent to the incoming L line. As already pointed out, due to the chosen SM Higgs insertion⁸, this model does not require any BSM scalar doublet. Completion of this model diagram is made by utilizing three BSM colored triplet scalars and two colored triplet fermions, which are all iso-singlets. See Fig. 13 and Table 5 for more details.

Note that if the color anti-triplets $\psi_1, \chi_{2,3}$ are replaced by color triplets in T2-ii-1-A(C), then a variation of this model can be constructed with ψ_2 being octet under $SU(3)_C$. A

⁸It is noteworthy to mention that attaching H at the outer scalar loop would require a colored triplet scalar which is an iso-doublet. By inserting H in this manner, two separate next-to-minimal models can be constructed depending on whether d_R or u_R is running in the internal fermion propagator adjacent to incoming L . However, we do not list these scenarios since they do not qualify to be the most minimal models.

similar variant model can emerge from T2-iii-1-A(C) if $\chi_{2,3}$ be the color triplets instead and ψ_2 being color octet under $SU(3)_C$.

□ T2-iv-1-A(C) & T2-v-2-A(C):

The fabrication process of T2-iv and T2-v are discussed at length in the previous section. It is pointed out that two of the internal scalar propagators connected to the fermions must be H and η , no other variation can be made to construct a viable two-loop model out of these skeleton diagrams. Due to this special property, the only two scalars that can carry color quantum numbers are χ and ω , as shown in Fig. 13. To satisfy the minimality conditions, these fields are chosen to be color triplets, see Table 5 for the complete quantum numbers of all the states associated to these models.

□ T2-vi-4-A(C):

Note that, for the scenario with color singlets, the minimal model is constructed out of T2-vi-3 diagram (Fig. 12), whereas, if particles carrying colors are allowed, no such vertex of the type $\psi\psi\sigma$ is allowed, since it cannot be invariant under $SU(3)_C$. This can only be done if two different fermions are used to form this vertex, hence fails to be minimal. Instead, we build the minimal model by making use of T2-vi-4 diagram (instead of T2-vi-3, see Fig. 12), which requires two singly charged scalars (instead of one), but the same number of BSM fermions as before. For minimality, three of the fermions that are allowed to carry color charge are taken to be triplets (or anti-triplets) under $SU(3)_C$. See Table 5 for more details.

4 Possible dark matter candidates

To generate neutrino mass, new particles must be added to the theory and we have presented many such examples in the previous two sections. From the theoretical point of view, it is very appealing, if the added particles needed to generate neutrino mass can also serve as DM candidates. Though our main focus of this work is to select minimal models of Dirac neutrino mass arising from generic one-loop and two-loop topologies constructed from the $d = 5$ effective operator of Eq. (1.2), in this section, we investigate the possibilities of having DM particles within these minimal scenarios. Since a DM particle cannot carry color, so we only concentrate on the models, where color singlet states are employed to generate neutrino mass.

In radiative neutrino mass models, DM particles can be incorporated, if additional symmetries beyond the SM are imposed. This idea was first proposed in Ref. [12] for Majorana neutrinos and known as *scotogenic* model. It was shown that a simple application of \mathcal{Z}_2 symmetry does the job, as long as, only BSM particles are circulating inside the loop. This \mathcal{Z}_2 symmetry must remain unbroken even after the breaking of EW symmetry.

In the framework we are working, the spontaneously broken $U(1)_{B-L}$ symmetry, may leave a residual unbroken symmetry that can potentially stabilize the DM particle. The nature of the unbroken residual symmetry $U(1)_{B-L} \rightarrow \mathcal{Z}_N$ depends on the details of the $B - L$ charge assignments of the scalars. In our set-up, since, the SM Higgs doublet H

Models	Residual lepton symmetry	Residual dark symmetry	Choice of Y	Possible DM candidate
T1-i-1-A	\mathcal{Z}_3	✗	—	✗
T1-i-1-B	\mathcal{Z}_3	✗	—	✗
T1-i-1-C	\mathcal{Z}_6	✓	—	$\psi_{L,R}, \eta, \phi$
T1-i-2-A	\mathcal{Z}_6	✓	0	$\psi_{L,R}, \phi, \eta_1, \eta_2$
			-1	ϕ
T1-i-2-B	\mathcal{Z}_6	✓	0	$\psi_{L,R}, \phi_1, \phi_2, \eta_1, \eta_2$
			-1	ϕ_1, ϕ_2
T1-i-3-A	\mathcal{Z}_3	✗	—	✗
T1-i-3-B	\mathcal{Z}_6	✓	—	$\psi_{1L,R}, \psi_{2L,R}, \phi$
T1-ii-1-A	\mathcal{Z}_6	✓	0	$\psi_{L,R}, \eta, \phi$
			-1	ϕ

Table 6: As an example, in this table, for models with undetermined α , we take $\alpha = n/2$, where n is an odd integer.

is neutral under $U(1)_{B-L}$, the nature of the unbroken symmetry is entirely determined by the charge of the singlet scalar σ . In scenarios, where all the particles carry integer $B-L$ charge, then $U(1)_{B-L} \rightarrow \mathcal{Z}_3$ is realized because, σ carries three units of $B-L$ charge. Models with $N = 3$ cannot stabilize the DM particle, if any, by only the residual symmetry. In fact, it has been shown [48, 54] that in scotogenic Dirac neutrino mass models, for any odd integer N , one can always write down operators that eventually lead to DM decays. We find that three out of eight one-loop models (see Table 6) and three out of nine two-loop models (see Table 7) have the \mathcal{Z}_3 residual lepton symmetry, and consequently, DM stability cannot be guaranteed by the residual symmetry alone.

On the contrary, in models where any of the particles is carrying a half-odd-integer $B-L$ charge, the rescaled charge of σ must be 6, hence the unbroken symmetry is $U(1)_{B-L} \rightarrow \mathcal{Z}_6$ instead of \mathcal{Z}_3 . In these models, this unbroken \mathcal{Z}_6 plays the role of residual dark symmetry, hence stabilizes the DM candidates. Most of the models presented in this work, permit such a choice of half-odd-integer $B-L$ charge and, consequently, naturally incorporates DM within the minimal set-up without the need of extending the particle content any further. It is interesting to note that in the two-loop models that allow the half-odd-integer $B-L$ charge assignment, DM candidate exists, even though SM fermions are propagating inside the loop, a feature that has been overlooked in the literature. List of the models and their associated residual symmetries and possible DM candidates are listed in Tables 6 and 7. In a future work [106], we plan to construct the minimal *scotogenic* one-loop and two-loop models of Dirac neutrino mass arising from this working framework and study their associated DM phenomenology in great details.

5 Conclusions

In this work, we have performed a systematic search for the minimal Dirac neutrino mass models that arise from generic one-loop and two-loop topologies constructed from the $d = 5$

Models	Residual lepton symmetry	Residual dark symmetry	Choice of Y	Possible DM candidate
T2-i-2-A	\mathcal{Z}_3	\times	—	\times
T2-i-4-A	\mathcal{Z}_3	\times	—	\times
T2-i-11-A	\mathcal{Z}_3	\times	—	\times
T2-ii-1-A	\mathcal{Z}_6	\checkmark	—	$\psi_{1L,R}, \eta_2$
T2-ii-2-A	\mathcal{Z}_6	\checkmark	—	$\psi_{2L,R}$
T2-iii-1-A	\mathcal{Z}_6	\checkmark	0	$\psi_{2L,R}$
			-1	η_2, η_3
T2-iv-1-A	\mathcal{Z}_6	\checkmark	$\frac{1}{2}$	ϕ, η
			$-\frac{1}{2}$	ϕ
T2-v-2-A	\mathcal{Z}_6	\checkmark	$\frac{1}{2}$	ϕ
			$-\frac{1}{2}$	ϕ, η_2
T2-vi-3-A	\mathcal{Z}_6	\checkmark	—	$\psi_{2L,R}, \psi_{4L,R}$

Table 7: As an example, in this table, for models with undetermined α , we take $\alpha = n/2$, where n is an odd integer.

effective operator: $\bar{L}\tilde{H}\nu_R\sigma$. Dirac nature of neutrinos is ensured by the $U(1)_{B-L}$ gauge extension of SM and with non-universal charge assignments of the right-handed neutrinos under it. After setting up our ground rules for minimality within the working framework, we have done an exhaustive analysis, case by case, to select economical models with and without colored particles propagating in the loop(s).

At one-loop level, out of the six possible topologies T1-x (x=i-vi), we have found only two topologies T1-i and T1-ii that can lead to viable minimal models for Dirac neutrinos. After filtering out the less economical models, we ended up finding seven minimal models from T1-i and a single model from T1-ii with color singlet states. The corresponding numbers are eight and one, when colored particles are employed to build models. The complete list of viable one-loop models are listed in Tables 2 and 3, and the representative neutrino mass generation diagrams are presented in Figs. 5 and 6.

In the two-loop scenario, there are essentially eighteen topologies that can generate a potentially very large number of diagrams. We thoroughly investigate the six basic diagrams T2-x (x=i-vi) that emerge from the generic topologies, and named them skeleton diagrams. As discussed in the text, many variations of models can be constructed from each of these skeleton diagrams. Our systematic procedure, discussed at great length, helped us selecting the associated minimal versions of the models. We have found three minimal models from T2-i, two from T2-ii and one each from T2-x with x=ii-vi skeleton diagrams by employing particles that do not carry color. When the internal particles are assumed to be non-singlets of color group, we have found nine minimal models from T2-i and one from each T2-x with x=ii - vi skeleton diagrams. The complete list of two-loop models is summarized in Tables 4 and 5, and the representative neutrino mass generation diagrams are shown in Figs. 10 and 13.

Furthermore, we have explored the possibilities of having DM candidates in each of

these models. In the one-loop models, where SM particles circulate in the loop, there is no prospect of having a DM particle. In the alternate scenario, where all BSM states are running inside the loop, appearance of DM candidate arise naturally. Out of the eight models without colored states, five of them can incorporate DM particles. Whereas for the two-loop models, six out of nine minimal models contain DM candidate. It is interesting to note that in the two-loop scenarios, even though, SM particles circulate in the loops, DM candidate can still be obtained as a result of emergent dark symmetry. The models with colored states do not lead to DM particles since, stable colored particles are experimentally excluded. In conclusion, dark matter candidate, naturally arises in most of the minimal models presented here, without extending the particle content any further. In our set-up, the stability of these DM particles are guaranteed by the residual dark symmetry emerging from the spontaneously breaking of the $U(1)_{B-L}$ symmetry.

In total, we have worked out forty unique minimal models. Whereas only a few of these models presented in this work are discussed in the literature before, most of the models are new. It is interesting to note that every single minimal model presented in this work with colored particles only require fundamental representation under $SU(3)_C$. Furthermore, for all models with or without colored particles, no representation higher than a fundamental representation of $SU(2)_L$ are employed either. Each of the models presented in this work can have very distinct and rich phenomenology and must be studied case by case, which is beyond the scope of this work. Following our detailed systematic approach presented in this work, new models of radiative Dirac neutrino mass can be constructed straightforwardly in different frameworks, such as by implementing alternative symmetries (discrete or continuous, for example $U(1)_R$ or general $U(1)_X$ theories) to forbid tree-level Dirac and Majorana mass terms at all orders.

Acknowledgments

We are grateful for helpful discussions with Kaladi Babu and Ernest Ma. This work was partially supported by the US Department of Energy Grant Number DE-SC 0016013 and also by the Neutrino Theory Network Program under Grant No. DE-AC02-07CH11359. SJ thanks the Fermilab Theory Group for warm hospitality during the completion of this work.

References

- [1] P. Minkowski, “ $\mu \rightarrow e\gamma$ at a Rate of One Out of 10^9 Muon Decays?,” *Phys. Lett.* **67B** (1977) 421–428.
- [2] T. Yanagida, “Horizontal gauge symmetry and masses of neutrinos,” *Conf. Proc.* **C7902131** (1979) 95–99.
- [3] M. Gell-Mann, P. Ramond, and R. Slansky, “Complex Spinors and Unified Theories,” *Conf. Proc.* **C790927** (1979) 315–321, [arXiv:1306.4669 \[hep-th\]](#).
- [4] R. N. Mohapatra and G. Senjanovic, “Neutrino Mass and Spontaneous Parity Nonconservation,” *Phys. Rev. Lett.* **44** (1980) 912.

- [5] J. Schechter and J. W. F. Valle, “Neutrino Masses in $SU(2) \times U(1)$ Theories,” *Phys. Rev.* **D22** (1980) 2227.
- [6] J. Schechter and J. W. F. Valle, “Neutrino Decay and Spontaneous Violation of Lepton Number,” *Phys. Rev.* **D25** (1982) 774.
- [7] R. Foot, H. Lew, X. G. He, and G. C. Joshi, “Seesaw Neutrino Masses Induced by a Triplet of Leptons,” *Z. Phys.* **C44** (1989) 441.
- [8] A. Zee, “A Theory of Lepton Number Violation, Neutrino Majorana Mass, and Oscillation,” *Phys. Lett.* **93B** (1980) 389. [Erratum: *Phys. Lett.* 95B,461(1980)].
- [9] A. Zee, “Quantum Numbers of Majorana Neutrino Masses,” *Nucl. Phys.* **B264** (1986) 99–110.
- [10] K. S. Babu, “Model of ‘Calculable’ Majorana Neutrino Masses,” *Phys. Lett.* **B203** (1988) 132–136.
- [11] K. S. Babu and E. Ma, “Natural Hierarchy of Radiatively Induced Majorana Neutrino Masses,” *Phys. Rev. Lett.* **61** (1988) 674.
- [12] E. Ma, “Verifiable radiative seesaw mechanism of neutrino mass and dark matter,” *Phys. Rev.* **D73** (2006) 077301, [arXiv:hep-ph/0601225](#) [hep-ph].
- [13] Y. Cai, J. Herrero-García, M. A. Schmidt, A. Vicente, and R. R. Volkas, “From the trees to the forest: a review of radiative neutrino mass models,” *Front.in Phys.* **5** (2017) 63, [arXiv:1706.08524](#) [hep-ph].
- [14] T. P. Cheng and L.-F. Li, “On Weak Interaction Induced Neutrino Oscillations,” *Phys. Rev.* **D17** (1978) 2375.
- [15] E. Ma and R. Srivastava, “Dirac or inverse seesaw neutrino masses with $B - L$ gauge symmetry and S_3 flavor symmetry,” *Phys. Lett.* **B741** (2015) 217–222, [arXiv:1411.5042](#) [hep-ph].
- [16] E. Ma, N. Pollard, R. Srivastava, and M. Zakeri, “Gauge $B - L$ Model with Residual Z_3 Symmetry,” *Phys. Lett.* **B750** (2015) 135–138, [arXiv:1507.03943](#) [hep-ph].
- [17] E. Ma and R. Srivastava, “Dirac or inverse seesaw neutrino masses from gauged BL symmetry,” *Mod. Phys. Lett.* **A30** no. 26, (2015) 1530020, [arXiv:1504.00111](#) [hep-ph].
- [18] J. W. F. Valle and C. A. Vaquera-Araujo, “Dynamical seesaw mechanism for Dirac neutrinos,” *Phys. Lett.* **B755** (2016) 363–366, [arXiv:1601.05237](#) [hep-ph].
- [19] S. Centelles Chuliá, E. Ma, R. Srivastava, and J. W. F. Valle, “Dirac Neutrinos and Dark Matter Stability from Lepton Quarticity,” *Phys. Lett.* **B767** (2017) 209–213, [arXiv:1606.04543](#) [hep-ph].
- [20] S. Centelles Chuliá, R. Srivastava, and J. W. F. Valle, “CP violation from flavor symmetry in a lepton quarticity dark matter model,” *Phys. Lett.* **B761** (2016) 431–436, [arXiv:1606.06904](#) [hep-ph].
- [21] M. Reig, J. W. F. Valle, and C. A. Vaquera-Araujo, “Realistic $SU(3)_c \otimes SU(3)_L \otimes U(1)_X$ model with a type II Dirac neutrino seesaw mechanism,” *Phys. Rev.* **D94** no. 3, (2016) 033012, [arXiv:1606.08499](#) [hep-ph].
- [22] S. Centelles Chuliá, R. Srivastava, and J. W. F. Valle, “Generalized Bottom-Tau unification, neutrino oscillations and dark matter: predictions from a lepton quarticity flavor approach,” *Phys. Lett.* **B773** (2017) 26–33, [arXiv:1706.00210](#) [hep-ph].

- [23] S. Centelles Chuliá, “Dirac neutrinos, dark matter stability and flavour predictions from Lepton Quarticity,” in *7th International Pontecorvo Neutrino Physics School Prague, Czech Republic, August 20-September 1, 2017*. 2017. [arXiv:1711.10719 \[hep-ph\]](#).
- [24] D. Borah and A. Dasgupta, “Naturally Light Dirac Neutrino in Left-Right Symmetric Model,” *JCAP* **1706** no. 06, (2017) 003, [arXiv:1702.02877 \[hep-ph\]](#).
- [25] C. Bonilla, J. M. Lamprea, E. Peinado, and J. W. F. Valle, “Flavour-symmetric type-II Dirac neutrino seesaw mechanism,” *Phys. Lett.* **B779** (2018) 257–261, [arXiv:1710.06498 \[hep-ph\]](#).
- [26] D. Borah and B. Karmakar, “ A_4 flavour model for Dirac neutrinos: Type I and inverse seesaw,” *Phys. Lett.* **B780** (2018) 461–470, [arXiv:1712.06407 \[hep-ph\]](#).
- [27] D. Borah and B. Karmakar, “Linear seesaw for Dirac neutrinos with A_4 flavour symmetry,” *Phys. Lett.* **B789** (2019) 59–70, [arXiv:1806.10685 \[hep-ph\]](#).
- [28] E. Ma, “ $U(1)_\chi$ and Seesaw Dirac Neutrinos,” [arXiv:1811.09645 \[hep-ph\]](#).
- [29] D. Borah, D. Nanda, and A. K. Saha, “Common origin of modified chaotic inflation, non thermal dark matter and Dirac neutrino mass,” [arXiv:1904.04840 \[hep-ph\]](#).
- [30] P.-H. Gu, “Double type-II seesaw accompanied by Dirac fermionic dark matter,” [arXiv:1907.10019 \[hep-ph\]](#).
- [31] J. Calle, D. Restrepo, and \tilde{A} . Zapata, “Dirac neutrino mass generation from Majorana messenger,” [arXiv:1909.09574 \[hep-ph\]](#).
- [32] R. N. Mohapatra, “A Model for Dirac Neutrino Masses and Mixings,” *Phys. Lett.* **B198** (1987) 69–72.
- [33] R. N. Mohapatra, “Left-right Symmetry and Finite One Loop Dirac Neutrino Mass,” *Phys. Lett.* **B201** (1988) 517–524.
- [34] B. S. Balakrishna and R. N. Mohapatra, “Radiative Fermion Masses From New Physics at Tev Scale,” *Phys. Lett.* **B216** (1989) 349–352.
- [35] G. C. Branco and G. Senjanovic, “The Question of Neutrino Mass,” *Phys. Rev.* **D18** (1978) 1621.
- [36] K. S. Babu and X. G. He, “Dirac Neutrino Masses As Two Loop Radiative Corrections,” *Mod. Phys. Lett.* **A4** (1989) 61.
- [37] P.-H. Gu and U. Sarkar, “Radiative Neutrino Mass, Dark Matter and Leptogenesis,” *Phys. Rev.* **D77** (2008) 105031, [arXiv:0712.2933 \[hep-ph\]](#).
- [38] Y. Farzan and E. Ma, “Dirac neutrino mass generation from dark matter,” *Phys. Rev.* **D86** (2012) 033007, [arXiv:1204.4890 \[hep-ph\]](#).
- [39] H. Okada, “Two loop Induced Dirac Neutrino Model and Dark Matters with Global $U(1)'$ Symmetry,” [arXiv:1404.0280 \[hep-ph\]](#).
- [40] C. Bonilla, E. Ma, E. Peinado, and J. W. F. Valle, “Two-loop Dirac neutrino mass and WIMP dark matter,” *Phys. Lett.* **B762** (2016) 214–218, [arXiv:1607.03931 \[hep-ph\]](#).
- [41] W. Wang and Z.-L. Han, “Naturally Small Dirac Neutrino Mass with Intermediate $SU(2)_L$ Multiplet Fields,” [arXiv:1611.03240 \[hep-ph\]](#). [JHEP04,166(2017)].
- [42] E. Ma and U. Sarkar, “Radiative Left-Right Dirac Neutrino Mass,” *Phys. Lett.* **B776** (2018) 54–57, [arXiv:1707.07698 \[hep-ph\]](#).

- [43] W. Wang, R. Wang, Z.-L. Han, and J.-Z. Han, “The $B - L$ Scotogenic Models for Dirac Neutrino Masses,” *Eur. Phys. J.* **C77** no. 12, (2017) 889, [arXiv:1705.00414 \[hep-ph\]](#).
- [44] J. C. Helo, M. Hirsch, and T. Ota, “Proton decay and light sterile neutrinos,” *JHEP* **06** (2018) 047, [arXiv:1803.00035 \[hep-ph\]](#).
- [45] M. Reig, D. Restrepo, J. W. F. Valle, and O. Zapata, “Bound-state dark matter and Dirac neutrino masses,” *Phys. Rev.* **D97** no. 11, (2018) 115032, [arXiv:1803.08528 \[hep-ph\]](#).
- [46] Z.-L. Han and W. Wang, “ Z' Portal Dark Matter in $B - L$ Scotogenic Dirac Model,” *Eur. Phys. J.* **C78** no. 10, (2018) 839, [arXiv:1805.02025 \[hep-ph\]](#).
- [47] S. K. Kang and O. Popov, “Radiative neutrino mass via fermion kinetic mixing,” *Phys. Rev.* **D98** no. 11, (2018) 115025, [arXiv:1807.07988 \[hep-ph\]](#).
- [48] C. Bonilla, S. Centelles-Chuliá, R. Cepedello, E. Peinado, and R. Srivastava, “Dark matter stability and Dirac neutrinos using only Standard Model symmetries,” [arXiv:1812.01599 \[hep-ph\]](#).
- [49] J. Calle, D. Restrepo, C. E. Yaguna, and Ó. Zapata, “Minimal radiative Dirac neutrino mass models,” *Phys. Rev.* **D99** no. 7, (2019) 075008, [arXiv:1812.05523 \[hep-ph\]](#).
- [50] C. D. R. Carvajal and Ó. Zapata, “One-loop Dirac neutrino mass and mixed axion-WIMP dark matter,” *Phys. Rev.* **D99** no. 7, (2019) 075009, [arXiv:1812.06364 \[hep-ph\]](#).
- [51] E. Ma, “Scotogenic $U(1)_\chi$ Dirac neutrinos,” *Phys. Lett.* **B793** (2019) 411–414, [arXiv:1901.09091 \[hep-ph\]](#).
- [52] P. D. Bolton, F. F. Deppisch, C. Hati, S. Patra, and U. Sarkar, “An alternative formulation of left-right symmetry with $B - L$ conservation and purely Dirac neutrinos,” [arXiv:1902.05802 \[hep-ph\]](#).
- [53] S. Saad, “Simplest Radiative Dirac Neutrino Mass Models,” *Nucl. Phys.* **B943** (2019) 114636, [arXiv:1902.07259 \[hep-ph\]](#).
- [54] C. Bonilla, E. Peinado, and R. Srivastava, “The role of residual symmetries in dark matter stability and the neutrino nature,” *LHEP* **124** (2019) 1, [arXiv:1903.01477 \[hep-ph\]](#).
- [55] A. Dasgupta, S. K. Kang, and O. Popov, “Radiative Dirac Neutrino Mass with Dark Matter and its implication to $0\nu 4\beta$ in the $U(1)_{B-L}$ extension of the Standard Model,” [arXiv:1903.12558 \[hep-ph\]](#).
- [56] S. Jana, V. P. K., and S. Saad, “Minimal Dirac Neutrino Mass Models from $U(1)_R$ Gauge Symmetry and Left-Right Asymmetry at Collider,” [arXiv:1904.07407 \[hep-ph\]](#).
- [57] K. Enomoto, S. Kanemura, K. Sakurai, and H. Sugiyama, “New model for radiatively generated Dirac neutrino masses and lepton flavor violating decays of the Higgs boson,” *Phys. Rev.* **D100** no. 1, (2019) 015044, [arXiv:1904.07039 \[hep-ph\]](#).
- [58] E. Ma, “Two-Loop Z_4 Dirac Neutrino Masses and Mixing, with Self-Interacting Dark Matter,” [arXiv:1907.04665 \[hep-ph\]](#).
- [59] D. Restrepo, A. Rivera, and W. Tangarife, “Singlet-Doublet Dirac Dark Matter and Neutrino Masses,” [arXiv:1906.09685 \[hep-ph\]](#).
- [60] G. 't Hooft, “Naturalness, chiral symmetry, and spontaneous chiral symmetry breaking,” *NATO Sci. Ser. B* **59** (1980) 135–157.
- [61] S. B. Giddings and A. Strominger, “Axion Induced Topology Change in Quantum Gravity and String Theory,” *Nucl. Phys.* **B306** (1988) 890–907.

- [62] S. B. Giddings and A. Strominger, “String Wormholes,” *Phys. Lett.* **B230** (1989) 46–51.
- [63] S. B. Giddings and A. Strominger, “Baby Universes, Third Quantization and the Cosmological Constant,” *Nucl. Phys.* **B321** (1989) 481–508.
- [64] L. F. Abbott and M. B. Wise, “Wormholes and Global Symmetries,” *Nucl. Phys.* **B325** (1989) 687–704.
- [65] S. R. Coleman and K.-M. Lee, “Wormholes Made without Massless Matter Fields,” *Nucl. Phys.* **B329** (1990) 387–409.
- [66] A. Davidson, “ $B - L$ as the Fourth Color, Quark - Lepton Correspondence, and Natural Masslessness of Neutrinos Within a Generalized W_5 Model,” *Phys. Rev.* **D20** (1979) 776.
- [67] R. E. Marshak and R. N. Mohapatra, “Quark - Lepton Symmetry and $B-L$ as the $U(1)$ Generator of the Electroweak Symmetry Group,” *Phys. Lett.* **91B** (1980) 222–224.
- [68] R. N. Mohapatra and R. E. Marshak, “Local $B-L$ Symmetry of Electroweak Interactions, Majorana Neutrinos and Neutron Oscillations,” *Phys. Rev. Lett.* **44** (1980) 1316–1319. [Erratum: *Phys. Rev. Lett.* **44**, 1643 (1980)].
- [69] C. Wetterich, “Neutrino Masses and the Scale of $B-L$ Violation,” *Nucl. Phys.* **B187** (1981) 343–375.
- [70] P. Langacker, “The Physics of Heavy Z' Gauge Bosons,” *Rev. Mod. Phys.* **81** (2009) 1199–1228, [arXiv:0801.1345 \[hep-ph\]](#).
- [71] J. C. Montero and V. Pleitez, “Gauging $U(1)$ symmetries and the number of right-handed neutrinos,” *Phys. Lett.* **B675** (2009) 64–68, [arXiv:0706.0473 \[hep-ph\]](#).
- [72] A. C. B. Machado and V. Pleitez, “Schizophrenic active neutrinos and exotic sterile neutrinos,” *Phys. Lett.* **B698** (2011) 128–130, [arXiv:1008.4572 \[hep-ph\]](#).
- [73] A. C. B. Machado and V. Pleitez, “Quasi-Dirac neutrinos in a model with local $B - L$ symmetry,” *J. Phys.* **G40** (2013) 035002, [arXiv:1105.6064 \[hep-ph\]](#).
- [74] E. Ma, “Pathways to naturally small neutrino masses,” *Phys. Rev. Lett.* **81** (1998) 1171–1174, [arXiv:hep-ph/9805219 \[hep-ph\]](#).
- [75] K. S. Babu and C. N. Leung, “Classification of effective neutrino mass operators,” *Nucl. Phys.* **B619** (2001) 667–689, [arXiv:hep-ph/0106054 \[hep-ph\]](#).
- [76] F. Bonnet, D. Hernandez, T. Ota, and W. Winter, “Neutrino masses from higher than $d=5$ effective operators,” *JHEP* **10** (2009) 076, [arXiv:0907.3143 \[hep-ph\]](#).
- [77] F. Bonnet, M. Hirsch, T. Ota, and W. Winter, “Systematic study of the $d=5$ Weinberg operator at one-loop order,” *JHEP* **07** (2012) 153, [arXiv:1204.5862 \[hep-ph\]](#).
- [78] S. S. C. Law and K. L. McDonald, “The simplest models of radiative neutrino mass,” *Int. J. Mod. Phys.* **A29** (2014) 1450064, [arXiv:1303.6384 \[hep-ph\]](#).
- [79] D. Aristizabal Sierra, A. Degee, L. Dorame, and M. Hirsch, “Systematic classification of two-loop realizations of the Weinberg operator,” *JHEP* **03** (2015) 040, [arXiv:1411.7038 \[hep-ph\]](#).
- [80] R. Cepedello, M. Hirsch, and J. C. Helo, “Loop neutrino masses from $d = 7$ operator,” *JHEP* **07** (2017) 079, [arXiv:1705.01489 \[hep-ph\]](#).
- [81] G. Anamiati, O. Castillo-Felisola, R. M. Fonseca, J. C. Helo, and M. Hirsch, “High-dimensional neutrino masses,” *JHEP* **12** (2018) 066, [arXiv:1806.07264 \[hep-ph\]](#).

- [82] R. Cepedello, R. M. Fonseca, and M. Hirsch, “Systematic classification of three-loop realizations of the Weinberg operator,” *JHEP* **10** (2018) 197, [arXiv:1807.00629 \[hep-ph\]](#). [erratum: JHEP06,034(2019)].
- [83] C. Klein, M. Lindner, and S. Ohmer, “Minimal Radiative Neutrino Masses,” *JHEP* **03** (2019) 018, [arXiv:1901.03225 \[hep-ph\]](#).
- [84] E. Ma and O. Popov, “Pathways to Naturally Small Dirac Neutrino Masses,” *Phys. Lett. B* **764** (2017) 142–144, [arXiv:1609.02538 \[hep-ph\]](#).
- [85] C.-Y. Yao and G.-J. Ding, “Systematic analysis of Dirac neutrino masses from a dimension five operator,” *Phys. Rev. D* **97** no. 9, (2018) 095042, [arXiv:1802.05231 \[hep-ph\]](#).
- [86] S. Centelles Chuliá, R. Srivastava, and J. W. F. Valle, “Seesaw roadmap to neutrino mass and dark matter,” *Phys. Lett. B* **781** (2018) 122–128, [arXiv:1802.05722 \[hep-ph\]](#).
- [87] C.-Y. Yao and G.-J. Ding, “Systematic Study of One-Loop Dirac Neutrino Masses and Viable Dark Matter Candidates,” *Phys. Rev. D* **96** no. 9, (2017) 095004, [arXiv:1707.09786 \[hep-ph\]](#). [Erratum: Phys. Rev.D98,no.3,039901(2018)].
- [88] S. Centelles Chuliá, R. Srivastava, and J. W. F. Valle, “Seesaw Dirac neutrino mass through dimension-six operators,” *Phys. Rev. D* **98** no. 3, (2018) 035009, [arXiv:1804.03181 \[hep-ph\]](#).
- [89] S. Centelles Chuliá, R. Cepedello, E. Peinado, and R. Srivastava, “Systematic classification of two loop $d = 4$ Dirac neutrino mass models and the Diracness-dark matter stability connection,” [arXiv:1907.08630 \[hep-ph\]](#).
- [90] I. Dorsner, S. Fajfer, and N. Kosnik, “Leptoquark mechanism of neutrino masses within the grand unification framework,” *Eur. Phys. J. C* **77** no. 6, (2017) 417, [arXiv:1701.08322 \[hep-ph\]](#).
- [91] S. Saad, “Origin of a two-loop neutrino mass from SU(5) grand unification,” *Phys. Rev. D* **99** no. 11, (2019) 115016, [arXiv:1902.11254 \[hep-ph\]](#).
- [92] C. Klein, M. Lindner, and S. Vogl, “Radiative neutrino masses and successful SU(5) unification,” [arXiv:1907.05328 \[hep-ph\]](#).
- [93] J. C. Pati and A. Salam, “Unified Lepton-Hadron Symmetry and a Gauge Theory of the Basic Interactions,” *Phys. Rev. D* **8** (1973) 1240–1251.
- [94] J. C. Pati and A. Salam, “Lepton Number as the Fourth Color,” *Phys. Rev. D* **10** (1974) 275–289. [Erratum: Phys. Rev.D11,703(1975)].
- [95] H. Georgi and S. L. Glashow, “Unity of All Elementary Particle Forces,” *Phys. Rev. Lett.* **32** (1974) 438–441.
- [96] H. Georgi, H. R. Quinn, and S. Weinberg, “Hierarchy of Interactions in Unified Gauge Theories,” *Phys. Rev. Lett.* **33** (1974) 451–454.
- [97] H. Georgi, “The State of the Art-Gauge Theories,” *AIP Conf. Proc.* **23** (1975) 575–582.
- [98] H. Fritzsch and P. Minkowski, “Unified Interactions of Leptons and Hadrons,” *Annals Phys.* **93** (1975) 193–266.
- [99] S. Dimopoulos and L. Susskind, “Mass Without Scalars,” *Nucl. Phys. B* **155** (1979) 237–252. [2,930(1979)].
- [100] S. Dimopoulos, “Technicolored Signatures,” *Nucl. Phys. B* **168** (1980) 69–92.

- [101] E. Farhi and L. Susskind, “Technicolor,” *Phys. Rept.* **74** (1981) 277.
- [102] B. Schrempp and F. Schrempp, “Naturally Light Leptoquarks,” *Phys. Lett.* **153B** (1985) 101–107.
- [103] R. Barbier *et al.*, “R-parity violating supersymmetry,” *Phys. Rept.* **420** (2005) 1–202, [arXiv:hep-ph/0406039](#) [[hep-ph](#)].
- [104] D. Abercrombie *et al.*, “Dark Matter Benchmark Models for Early LHC Run-2 Searches: Report of the ATLAS/CMS Dark Matter Forum,” [arXiv:1507.00966](#) [[hep-ex](#)].
- [105] K. S. Babu, P. S. B. Dev, S. Jana, and A. Thapa, “Non-Standard Interactions in Radiative Neutrino Mass Models,” [arXiv:1907.09498](#) [[hep-ph](#)].
- [106] S. Jana, V. P. K., and S. Saad, “Minimal One-loop and Two-loop Scotogenic Dirac Neutrino Mass Models from Gauged $U(1)_{B-L}$ Symmetry and Associated Dark Phenomenology,” (*in preparation*) .